Spring 5-5-2018

The Role of Hippo Pathway in Mitosis and Cancer

Xingcheng Chen
University of Nebraska Medical Center

THE ROLE OF HIPPO PATHWAY IN MITOSIS AND CANCER

by

Xingcheng Chen

A DISSERTATION

Presented to the Faculty of
the University of Nebraska Graduate College
in Partial Fulfillment of the Requirements
for the Degree of Doctor of Philosophy

Pathology & Microbiology Graduate Program

Under the Supervision of Professor Jixin Dong

University of Nebraska Medical Center
Omaha, Nebraska

October, 2017

Supervisory Committee:

Jennifer Black, Ph.D. Vimla Band, Ph.D.

Kaihong Su, Ph.D.

ACKNOWLEDGEMENTS

Funding support:

The China Scholarship Council; National Cancer Institute (NCI/NIH); Department of Defense; the COBRE Grant from the Nebraska Center for Cell Signaling/National Institute of General Medical Sciences (NIGMS/NIH).

Much more important than funding support, I would like to acknowledge the support and encouragement I received during my doctoral research.

First and foremost, I want to thank my advisor Dr. Jixin Dong for supporting me during my Ph.D training. Under his guidance, I equipped with a solid foundation not only for molecular biology techniques, but also cancer research insights. He has given me the freedom to pursue various projects and provided me with insightful discussions and suggestions about the research. Additionally, he led our group towards a happy family, in which we treat our labmates friendly, honestly and gratefully.

I also want to thank the members of my PhD committee, Dr. Vimla Band, Dr, Jennifer Black, and Dr. Kaihong Su for their helpful career advices and suggestions. I deeply appreciate their insightful suggestion and critical comments which greatly improved my scientific knowledge. Besides, I would also thank our collaborators, Dr. Pankaj Singh and his postdoctoral research fellow Dr. Surendra Shukla for their contributions and suggestion to the third chapter of my thesis.

I will forever be thankful to my previous and present lab members: Shuping Yang, Lin Zhang, Yuanhong Chen, Seth Stauffer, Jiuli Zhou, Yongji Zeng, Yu Ou, and Zhan Wang. Specifically, thank Yuanhong for supporting us in research needs and experience, and laboratory management; thank other colleagues for providing technique solutions as well as scientific suggestions on my research projects.

A sincere THANK YOU to my friends and families near and far. I especially thank my parents who provided me with unconditional love, and taught me to be a brave, self-confident, and hardworking person. Last but by no mean the least, the best outcome from these past five years is finding my best friend, soul-mate, and husband. I married the best person out there for me. I truly thank Xiangmin for sticking by my side, even when I was irritable and depressed.

I am so grateful for those who support me along the way of my Ph.D training.

ABSTRACT: THE ROLE OF HIPPO PATHWAY IN MITOSIS AND CANCER

Xingcheng Chen, Ph.D.

University of Nebraska, 2017

Supervisor: Jixin Dong, Ph.D.

The Hippo signaling pathway has been recently elucidated as a tumor suppressor pathway controlling cell proliferation and apoptosis. The core of this pathway is a kinase cascade which contains MST1/2 (Mammalian sterile 20-like kinase 1/2), LATS1/2 (large tumor suppressor 1/2) and downstream effector named Yes-associated protein (YAP). MST1/2 transduce their kinase activity mainly through directly phosphorylating LATS1/2. Once phosphorylated and activated, LATS1/2 subsequently phosphorylate and inhibit YAP from translocating to nucleus. Current studies involving the Hippo pathway focus on determining its oncogenic role in various organs/tissues. While those studies provide important insight into the tumor suppressor properties of this pathway, the underlying molecular mechanisms through which the Hippo components exert their oncogenic/suppressing function are poorly understood. Our study found that the adaptor protein Ajuba (recent found as a positive regulator of YAP oncogenic activity) and MST2 (the core kinase in the Hippo pathway), are phosphorylated by CDK1 in mitosis via novel sites. We further characterized the phospho-regulation of Ajuba and MST2 in mitosis and examined the functional significance of the phosphorylation. Mutation of those phosphorylation sites impact cell proliferation *in vitro* and tumorigenesis *in vivo*.

Our group has recently shown that the downstream effector of the Hippo pathway, YAP, is phosphorylated during mitosis and activated in a CDK1-dependent manner. In this study, we generated, for the first time, a doxycycline-inducible mouse model in which

active YAP was specifically expressed in the pancreas. Interestingly, this mouse model develops pancreatic acinar-to-ductal metaplasia (ADM) in two weeks. Moreover, significant body weight loss and food intake decrease were observed after YAP induction in the pancreas, which are characteristics of cachexia. Cachexia is a wasting syndrome associated with typical types of cancer, particularly the gastrointestinal tract cancer and lung cancer. Among those cancer types, pancreatic ductal adenocarcinoma (PDAC) has the highest incidence of cancer cachexia. Therefore, our study suggests a potential role of YAP in pancreatic cancer-associated cachexia (CAC).

TABLE OF CONTENT

Acknowledgements i

Abstract: THE ROLE OF HIPPO PATHWAY IN MITOSIS AND CANCER iii

LIST OF FIGURES AND TABLES x

LIST OF ABBREVIATIONS x

Chapter 1: Ajuba Phosphorylation by CDK1 Promotes Cell Proliferation and Tumorigenesis* 1

Abstract 2

1.1. Introduction 3

1.2. Materials and Methods 6

1.2.1. Cell Culture and Transfection 6

1.2.2. Expression Constructs 7

1.2.3. Tet-On-inducible Expression System 7

1.2.4. Quantitative Real-time PCR 8

1.2.5. Recombinant Protein Purification and in Vitro Kinase Assay 8

1.2.6. Antibodies 8

1.2.7. Phos-tag and Western Blot Analysis 9

1.2.8. Immunofluorescence Staining and Confocal Microscopy 10

1.2.9. Colony Formation and Cell Proliferation Assays 10

1.2.10. Animal Studies 10

1.2.11. Statistical Analysis 11

1.3. Results 12

1.3.1. Ajuba Family Proteins Are Phosphorylated during Antimitotic Drug-induced G2/M Arrest 12

1.3.2. Identification of the Corresponding Kinase for Ajuba Phosphorylation 12
1.3.3. CDK1 Phosphorylates Ajuba in Vitro 13
1.3.4. CDK1-Cyclin B Complex Phosphorylates Ajuba at Ser 119 in Vitro and in Cells 13
1.3.5. CDK1/Cyclin B Mediates Ajuba Phosphorylation at Ser119 and Ser175 in Cells 14
1.3.6. Ajuba Phosphorylation Occurs during Normal Mitosis.....15
1.3.7. Mitotic Phosphorylation of Ajuba Impacts Cell Cycle Regulators without Affecting YAP Activity 15
1.3.8. Mitotic Phosphorylation of Ajuba Is Required for Cell Proliferation and Anchorage-independent Growth 17
1.3.9. Mitotic Phosphorylation of Ajuba Is Required for Tumorigenesis.....18
1.4. Discussion 19

Chapter 2: MST2 phosphorylation at serine 385 in mitosis inhibits its tumor suppressing activity 36

Abstract.....37
2.1. Introduction.....38
2.2. Materials and Methods 40
2.2.1. Expression constructs, cell culture and transfection.....40
2.2.2. Tet-On-inducible expression system.....40
2.2.3. Recombinant protein purification and in vitro kinase assay 41
2.2.4. Antibodies.....41
2.2.5. Phos-tag and Western blot analysis.....42
2.2.6. Cell proliferation and colony formation assays.....42
2.2.7. Animal studies analysis 42

2.2.8. Statistical analysis 43
2.3. Results 44
2.3.1. MST2 is phosphorylated during antimitotic drug-induced G2/M arrest 44
2.3.2. Identification of the corresponding kinase for MST2 phosphorylation....44
2.3.3. CDK1 phosphorylates MST2 in vitro 45
2.3.4. CDK1/cyclin B complex phosphorylates MST2 at S385 in vitro....45
2.3.5. CDK1 phosphorylates MST2 at S385 in cells....46
2.3.6. MST2 phosphorylation on Ser385 occurs during normal mitosis....46
2.3.7. Mitotic phosphorylation of MST2 does not impact Hippo-YAP activity....46
2.3.8. The non-phosphorylatable mutant MST2 possesses stronger inhibitory activity in cell proliferation and anchorage-independent growth 47
2.3.9. The non-phosphorylatable MST2 mutant inhibits tumorigenesis in vivo 47
2.4. Discussion 49
Chapter 3: Role of YAP in Pancreatic Cancer-Associated Cachexia....63
ABSTRACT....64
3.1. Introduction....65
3.2. Materials and Methods 68
3.2.1. Generation of mouse strains....68
3.2.2. Immunohistochemistry (IHC) Staining....68
3.2.3. CXCL13 ELISA measurements....69
3.2.4. Statistical analysis 69
3.3. Results 70
3.3.1. YAP is sufficient to promote ADM in YAP-pancreas model. 70
3.3.2. The YAP-pancreas model has cachectic phenotype. 71
3.3.3. Association between YAP and CXCL13 in pancreatic CAC. 71

3.4. Discussion 73

BIBLIOGRAPHY..85

LIST OF FIGURES AND TABLES

Figure 1-1. CDK1-dependent phosphorylation of Ajuba during G2/M arrest. 22

Figure 1-2. Ajuba is phosphorylated by CDK1 in vitro and in cells 24

Figure 1-3. CDK1 mediates the phosphorylation of Ajuba at Ser119 and Ser175 during G2/M phase arrest. 26

Figure 1-4. Ajuba is phosphorylated at Ser119 and Ser175 during unperturbed time points and subjected to Western blotting analysis. 28

Figure 1-5. Mitotic phosphorylation controls the expression of cell cycle regulators, but does not affect the Hippo-YAP activity. 30

Figure 1-6. Mitotic phosphorylation of Ajuba is required for cell proliferation and anchorage-independent growth.....32

Figure 1-7. Ajuba phosphorylation is essential for tumorigenesis in mice. 34

Figure 2-1. CDK1-dependentphosphorylation of MST2 duringG2/M arrest. 51

Figure 2-2. CDK1 phosphorylates MST2 in vitro.....53

Figure 2-3. CDK1 mediates the phosphorylation of MST2 S385 in cells. 55

Figure 2-4. Mitotic phosphorylation of MST2 does not affect the Hippo-YAP activity. 57

Figure 2-5. MST2-S385A suppresses cell proliferation and anchorage-independent growth.....59

Figure 3-1. Generation of inducible pancreas-specific YAP overexpression. 76

Figure 3-2. YAP is sufficient for ADM in YAP-Pancreas model….....71

Figure 3-3. The YAP-Pancreas model has cachectic phenotype.. 73

Figure 3-4. CXCL13 is critical in YAP mediated pancreatic CAC.. 75

Table 1. List of genetic mouse strain source.....76

LIST OF ABBREVIATIONS

EMT	epithelial-mesenchymal transition
ADM	acinar-to-ductal metaplasia
BCA-1	B cell-attracting chemokine 1
BUB1	budding uninhibited by benzimidazoles 1
CAC	cancer-associated cachexia
CDC25C	cell division cycle 25C
CDK1	cyclin-dependent kinase 1
CK19	cytokeratin 19
CTGF	connective tissue growth factor
Cyr61	cysteine rich angiogenic inducer 61
DOX	doxycycline
ERK1	extracellular signal-regulated kinases
FBS	fetal bovine serum
FFA	free fatty acids
FRMD6	FERM Domain Containing 6
GPCR	G-protein coupled receptor
H&E	hematoxylin and eosin
HPNE	hTERT-immortalized human pancreatic nestin-expressing cell
IL-6	Interleukin 6
JNK1	c-Jun N-terminal protein kinase 1
JNK2	c-Jun N-terminal protein kinase 2

KIBRA	kidney and brain expressed protein
Lats1/2	large tumor suppressor 1/2
LIMD1	LIM-domain containing protein 1
MDSC	myeloid-derived suppressor cells
MEK1	MAP kinase/ ERK kinase 1
Mob1	mps one binder 1
MST1/2	mammalian sterile 20-like kinase 1/2
NDR1	N-myc downstream regulated 1
Nek2A	NIMA related kinase 2A
NF2	neurofibromatosis type 2
Noco	Nocodazole
PanIN	pancreatic intraepithelial neoplasia
PCR	polymerase chain reaction
PDAC	pancreatic ductal adenocarcinoma
PLK1	polo-like kinase 1
PTPN14	protein tyrosine phosphatase, non-receptor type 14
Sav	Protein Salvador Homolog 1
Ser	Serine
STK	serine/threonine kinases
Taxol	paclitaxel
TAZ	transcriptional co-activator with PDZ-binding motif
TEAD1	TEA domain family member 1

TGF-β	transforming growth factor beta
TICAMs	tumor initiating cells-associated macrophages
TICs	tumor- initiating cells
TIL-Bs	tumor-infiltrating lymphocytic B cells
WTIP	Wilms tumor 1 interacting protein
WW45	WW domain-containing protein, 45-kDa molecular mass
YAP	yes-associated protein
Yki	Yorkie

CHAPTER 1: AJUBA PHOSPHORYLATION BY CDK1 PROMOTES CELL PROLIFERATION AND TUMORIGENESIS*

*The material presented in this chapter was previously published: Chen et al. J Biol Chem 2016; 291(28): 14761-14772.

ABSTRACT

Recent studies identified the adaptor protein Ajuba as a positive regulator of Yes-associated protein (YAP) oncogenic activity through inhibiting large tumor suppressor (Lats1/2) core kinases of the Hippo pathway, which plays important roles in cancer. In this study, we define a novel mechanism for phospho-regulation of Ajuba in mitosis and its biological significance in cancer. We found that Ajuba is phosphorylated *in vitro* and *in vivo* by cyclin-dependent kinase 1 (CDK1) at Ser^{119} and Ser^{175} during the G2/M phase of the cell cycle. Mitotic phosphorylation of Ajuba controls the expression of multiple cell cycle regulators; however, it does not affect Hippo signaling activity, nor does it induce epithelial-mesenchymal transition (EMT). We further showed that mitotic phosphorylation of Ajuba is sufficient to promote cell proliferation and anchorage-independent growth in vitro and tumorigenesis in vivo. Collectively, our discoveries reveal a previously unrecognized mechanism for Ajuba regulation in mitosis and its role in tumorigenesis.

1.1. Introduction

Genetic screens in Drosophila have discovered the Hippo pathway [1] and extensive studies have demonstrated important roles for Hippo signaling in tissue homeostasis, stem cell function, and cancer biology [2-5]. Protein kinases MST1/2 (together with the adaptor protein WW45) and Lats1/2 (with the regulatory subunit Mob1) form the core complexes in the Hippo pathway and these proteins regulate each other through phosphorylation. This core kinase signaling subsequently phosphorylates and inactivates the downstream effectors, oncoproteins YAP and TAZ, by sequestering them in the cytoplasm and promoting ubiquitination-dependent degradation [4, 6]. During past years, many regulators and input signals have been identified that influence Hippo-YAP signaling activity, such as the cell polarity and adherens junctions proteins, mechanical force, actin cytoskeleton [6-8], hypoxia [9], energy stress [10, 11], and mitosis/cytokinesis stress [12-15]. The downstream effectors YAP/TAZ also cross-talk with, or function as, mediators of many other signaling pathways, such as the GPCRs, Wnt/ β-catenin, TGF-β/SMAD, EGF, Notch, Hedgehog, and KRas/MAPK pathways [16].

A previous study identified Drosophila jub (Djub, orthologous to Ajuba proteins in mammals) as a negative regulator of the Hippo pathway [17]. Djub promotes Yki (Drosophila ortholog of YAP/TAZ) activation through interacting with, and inhibiting, Warts (Drosophila ortholog of Lats1/2) kinase, and this function/mechanism appears to be conserved in mammalian cells [17]. Subsequent studies revealed that Ajuba functions as an adaptor protein that links EGFR-MAPK signaling to the Hippo pathway in both Drosophila and mammals [18]. Furthermore, Djub/Ajuba are also required for JNK-mediated activation of Yki/YAP, implying a conserved link between JNK signaling and Hippo pathway [19]. Interestingly, cytoskeletal tension modulates organ growth through

Yki in a Djub-dependent manner in Drosophila, although such a link in mammalian cells has not been identified [20].

Ajuba family proteins, including Ajuba, LIM-domain containing protein 1 (LIMD1), and Wilms tumor 1 interacting protein (WTIP), are adaptor/scaffold proteins with three LIM domains at their C termini. The LIM domains interact with other proteins in various subcellular locations to exert the biological functions of Ajuba proteins [21]. The Ajuba family is involved in many cellular processes such as cell-cell adhesion, gene transcription, cell proliferation, cell migration, and mitosis/cytokinesis [21]. Interestingly, several studies also suggest that Ajuba family proteins function as potential tumor suppressors or oncoproteins [22-26]. Some reports indicate that Ajuba is a critical member of the mitotic machinery. For example, Ajuba activates Aurora-A kinase to recruit the CDK1-cyclin B complex to centrosomes, and it contributes to mitotic entry [27]. Similarly, Ajuba associates with Lats2 at centrosomes during mitosis and regulates the integrity of the spindle apparatus [28]. Ajuba is also a microtubule-associated protein and plays a role in metaphase-anaphase transition through interactions with Aurora-B and BubR1 at kinetochores [29]. Collectively, these studies suggest an important role of Ajuba in mitosis, and indicate that Ajuba may exert its oncogenic or tumor suppressive function via dysregulation of mitosis. Ajuba has been observed to be phosphorylated by Aurora-A [27] and Lats2 [28] in mitosis; however, the phosphorylation site(s) and its biological function have remained elusive.

We have recently investigated how the Hippo pathway (core members and their regulators) is regulated in mitosis. We have shown that KIBRA (an upstream regulator of the Hippo pathway) [30, 31], YAP [12, 13], and TAZ [15] are phosphorylated by mitotic kinases. Importantly, mitotic phosphorylation of YAP/TAZ is critical for proper mitotic progression and for their oncogenic activity in cancer cells [12, 13, 15]. These studies

prompted us to further examine whether other components or regulators of the Hippo pathway are regulated by phosphorylation during mitosis. In this study, we found that many of the Hippo members/regulators, including Ajuba, are indeed phosphorylated during antimitotic drug-induced G2/M phase arrest. We characterized the phospho-regulation of Ajuba in mitosis, and identified CDK1 as a major kinase for mitotic-phosphorylation of Ajuba. We further examined the functional significance of the phosphorylation and found that mitotic-phosphorylation promotes the oncogenic activity of Ajuba independently of the Hippo pathway, suggesting a novel mechanism that regulates Ajuba in cancer cells.

1.2. Materials and Methods

1.2.1. Cell Culture and Transfection

HEK293T, HEK293GP, and HeLa cell lines were purchased from American Type Culture Collection (ATCC) and cultured as ATCC instructed. HPNE cells were provided by Dr. Michel Ouellette (University of Nebraska Medical Center, who established and deposited this cell line at ATCC) and were cultured as described [32].The cell lines were authenticated at ATCC and were used at low (<25) passages. The colon cancer cell line RCA was a gift from Dr. Michael Brattain (University of Nebraska Medical Center) [33] and was maintained in minimal essential medium supplemented with 10% FBS and antibiotics. Attractene (Qiagen) was used for transient overexpression of proteins in HEK293T and HEK293GP cells following the manufacturer's instructions. Ectopic expression of Ajuba or its mutants in HPNE cells was achieved by a retrovirus-mediated approach. Retrovirus packaging, infection, and subsequent selection were done as we have described previously [34]. Nocodazole (100ng/ml for 16h) and Taxol (100 n M for 16h) (Selleck Chemicals) were used to arrest cells in G2/M phase unless otherwise indicated. VX680 (Aurora-A,-B, and-C inhibitor), ZM447439 (Aurora-B,-C inhibitor), BI2536 (Plk1 inhibitor), Purvalanol A (CDK1/2/5 inhibitor), SB216763 (GSK-3β inhibitor), Rapamycin (mechanistic target of rapamycin inhibitor), and MK2206 (Akt inhibitor) were also from Selleck Chemicals. RO3306 (CDK1 inhibitor) and Roscovitine (CDK1/2/5 inhibitor) were from ENZO Life Sciences. MK5108 (Aurora-A inhibitor) was from Merck. Kinase inhibitors for MEK-ERK (with U0126), p38 (with SB203580), and PI-3K (with LY294002) were from LC Laboratory. All other chemicals were either from Sigma or ThermoFisher.

1.2.2. Expression Constructs

The human Ajuba cDNA clone (ID HSCD00323154) was obtained from Harvard Medical School. To make the retroviral or GFP-tagged Ajuba expression constructs, the above full-length cDNA was cloned into the MaRXTM IV [34] or pEGFP-C1 vector (Clontech), respectively. HA-FRMD6 (HA-EX) was made by cloning FRMD6 cDNA [35] into the pcDNA3.1-HA vector [34]. Myc-Lats2 has been described [34]. Point mutations were generated by the QuikChange Site-directed PCR mutagenesis kit (Stratagene) and verified by sequencing.

1.2.3. Tet-On-inducible Expression System

Tet-On-inducible shRNA vectors against Ajuba were purchased from GE Healthcare/Dharmacon (V3THS-343741). To make the shRNA-resistant (shR) Ajuba cDNA, the target sequence (5'-ACCGACTACCACAAAAATT-3') was changed into 5'-ACgGAtTAtCAtAAAAATT-3' by PCR mutagenesis. The mutated Ajuba cDNA was then cloned into the Tet-All vector [36] to generate a Tet-On-inducible shR-Ajuba construct. Ajuba down-regulationin RCA cells was achieved by lentivirus-mediated Ajuba shRNA expression in a doxycycline-dependent manner. Lentivirus generation and infection were performed as described with slight modifications [37]. The transduced cells were selected with puromycin (1 μg/ml) to establish pooled cell lines. The cell line in which the lack of Ajuba expression was confirmed (Tet-inducible knockdown) was then used for transduction/infection with virus expressing Tet-All-shR Ajuba or mutant constructs. Cells were maintained in medium containing Tet system-approved fetal bovine serum (Clontech Laboratories).

1.2.4. Quantitative Real-time PCR

Total RNA isolation, RNA reverse transcription, and quantitative real time-PCR were done as we have described previously [34].Cell proliferation analysis Cell numbers were monitored with an Invitrogen Countess automated cell counter after YAP was knocked down or overexpressed for 5 d. Trypan blue was used to identify and quantify viable cells.

1.2.5. Recombinant Protein Purification and in Vitro Kinase Assay

The GST-tagged Ajuba (amino acids 2–240, cloned in pGEX-5X-1) proteins were bacterially expressed and purified on GSTrap FF affinity columns (GE Healthcare) following the manufacturer's instructions. To make His-tagged Ajuba (amino acids 2-468), the corresponding Ajuba cDNA was subcloned into the pET-28a vector (Novagen/EMD Chemicals). The proteins were expressed and purified on HisPur^{TM} Cobalt spin columns (Pierce) following the manufacturer's instructions.

His-or GST-Ajuba (0.5-1 μg) was incubated with 5-10 units of recombinant CDK1/cyclin B complex (New England Biolabs) or 50-100 ng of CDK1/cyclinB (SignalChem) or HeLa cell total lysates (treated with DMSO or Taxol) in kinase buffer (New England Biolabs) in the presence of 5 μCi of [γ-^{32} P] ATP (3000 Ci/mmol, PerkinElmer Life Sciences). Phosphorylation (^{32}P incorporation) was visualized by autoradiography followed by Western blotting or detected by phospho-specific antibodies.

1.2.6. Antibodies

The polyclonal Ajuba antibodies (4897) from Cell Signaling Technology were used for Western blotting throughout the study. Rabbit polyclonal phospho-specific anti-bodies against human Ajuba Ser^{119} and Ser^{175} were generated and purified by AbMart. The peptides used for immunizing rabbits were TAPAL-pS-PRSSF (Ser^{119}) and DQRHG-pS-

PLPAG (Ser^{175}). The corresponding non-phosphorylated peptides were also synthesized and used for antibody purification and blocking assays. HA antibodies were from Sigma (H9658). Anti-β-actin (SC-47778), anti-GFP (SC-9996), and anti-cyclin B (SC-752) antibodies were from Santa Cruz Biotechnology. Aurora-A (A300-070A), glutathione S-transferase (GST) (A190-122A), His (A190-114A), MST1 (A300-465A), MST2 (A300-467A), Lats1 (A300-478A), Aurora B (A300-431A), BUB1 (A300-373A), and BubR1 (A300-386A) antibodies were from Bethyl Laboratories. Phospho-Thr^{288} /Thr^{232} /Thr^{198} Aurora-A/B/C (2914), Phospho-Histone H3 (Ser^{10}) (3377), phospho-Ser^{127} YAP (4911), phospho-Ser^{909} Lats1 (9157), Lats2 (5888), WW45 (3507), TAZ (4883), TEAD1 (12292), NF2 (6995), Vimentin (5741), E-cadherin (3195), PTPN14 (13808), LIMD1 (13245), Zyxin (3553), CDC25C (4688), CDK1 (9116), phos-pho-Tyr^{15} CDK1 (9111), cyclin A (4656), cyclin E (4132), p53 (2527), MAD2 (4636), phospho-Ser^{795} Rb(9301), and phospho-Ser^{642} Wee1 (4910) antibodies were also from Cell Signaling Technology. The monoclonal antibody against KIBRA has been described [34]. Rabbit anti-α-tubulin (Abcam, 15246) and mouse anti-β-tubulin (Sigma, T5293) antibodies were used for immunofluorescence staining.

1.2.7. Phos-tag and Western Blot Analysis

Phos-tag ™ was obtained from Wako Pure Chemical Industries, Ltd. (30493521) and used at 20 μM (with 100μM $MnCl_2$) in 6 or 8% SDS-acrylamide gels. Prior to transferring, the gels were equilibrated in transfer buffer containing 10 m M EDTA, two times, each for 10 min. The gels were then soaked in transfer buffer (without EDTA) for another 10 min. Western blotting, immunoprecipitation, and λ-phosphatase treatment assays were done as previously described [31].

1.2.8. Immunofluorescence Staining and Confocal Microscopy

Cell fixation, permeabilization, fluorescence staining, and microscopy were done as previously described [38]. For peptide blocking, a protocol from the Abcam website was used, as we previously described [12].

1.2.9. Colony Formation and Cell Proliferation Assays

Colony formation assays in soft agar were performed as described [32]. Cells (10,000/well) were seeded in a 6-well plate and colonies were counted by ImageJ online. For cell proliferation assays, cells (100,000/well) were seeded in a 6-well plate in triplicate. Cells were counted by a hemacytometer and proliferation curves were made based on the cell number in each well from three independent experiments.

1.2.10. Animal Studies

For in vivo xenograft studies, RCA cells (with Tet-shRNA-Ajuba) expressing Tet-All-shR-Ajuba or Tet-All-shR-Ajuba-2A (non-phosphorylatable mutant) (2.0×10^6 cells each line) were subcutaneously injected into the left or right flank of 6-week-old male athymic nude mice (Ncr-nu/nu, Harlan). Ten animals were used per group. Tumor sizes were measured once a week using an electronic caliper starting at 3 weeks after injection (when tumors in the Ajuba-2A group are palpable). Tumor volume (V) was calculated by the formula: $V = 0.5 \times \text{length} \times \text{width}^2$ [32]. Mice were euthanized at 6 weeks post-injection and the tumors were excised for subsequent analysis. The animals were housed in pathogen-free facilities. All animal experiments were approved by the University of Nebraska Medical Center Institutional Animal Care and Use Committee.

1.2.11. Statistical Analysis

Statistical significance was analyzed using a two-tailed, unpaired Student's t test.

1.3. Results

1.3.1. Ajuba Family Proteins Are Phosphorylated during Antimitotic Drug-induced G2/M Arrest

To further explore whether members of the Hippo pathway are regulated by phosphorylation during mitosis, we examined the phosphorylation status of the Hippo pathway proteins during G2/M arrest induced by Taxol or Nocodazole. As shown in Fig.1-1A, consistent with previous reports, there was a dramatic up-shift of Lats1 and Lats2 mobility (due to mitotic phosphorylation) [39] during Taxol or Nocodazole treatment (Fig. 1-1A). As expected, the mobility of KIBRA, YAP, and TAZ were all significantly retarded due to phosphorylation during G2/M arrest (Fig. 1-1A) [12, 15, 30, 31]. Taxol or Nocodazole treatment did not cause any evident change in the mobility/phosphorylation for PTPN14, NF2, or EX (which are all upstream regulators of the Hippo-YAP pathway), for WW45 or TEAD1 (Fig. 1-1A). Interestingly, MST2, but not MST1, was phosphorylated during G2/M arrest (Fig. 1-1A). One of the most prominent changes we observed was the striking mobility up-shift of the Ajuba and Zyxin family proteins including Ajuba, LIMD1, and Zyxin (Fig. 1-1A). In this study, we have chosen to focus on Ajuba, and so we further investigated its phosphorylation status. λ-Phosphatase treatment completely converted all slow-migrating bands to fast-migrating bands, confirming that the mobility shift of Ajuba during G2/M arrest is caused by phosphorylation (Fig. 1-1B).

1.3.2. Identification of the Corresponding Kinase for Ajuba Phosphorylation

Next, we used various kinase inhibitors to identify the candidate kinase for Ajuba phosphorylation. In contrast to the findings in a previous study [27], our data demonstrated that inhibition of Aurora-A (with MK5108) or Aurora-A, -B, and -C (with VX680) kinases only mildly reduced Ajuba phosphorylation (Fig.1-1C). Addition of BI2536 (an inhibitor for

mitotic kinase Plk1) had no effect on the Ajuba mobility shift/phosphorylation (Fig. 1-1C). Interestingly, treatments with RO3306 (CDK1inhibitor), Roscovitine (inhibits CDK1/2/5), or Purvalanol A (CDK1/2/5 inhibitor) almost completely reverted the mobility shift/phosphorylation (Fig. 1-1C, lanes 7-9). CDK1 is a well-known mitotic kinase. These data suggest that CDK1 is likely the corresponding kinase for Ajuba phosphorylation induced by Taxol or Nocodazole treatments. Inhibition of MEK-ERK kinases (with U0126), p38 (with SB203580),GSK-3β (with SB216763), mechanistic target of rapamycin (with rapamycin), PI-3K (with LY294002), or Akt (MK2206) failed to alter the phosphorylation of Ajuba during G2/M arrest (data not shown).

1.3.3. CDK1 Phosphorylates Ajuba in Vitro

To determine whether CDK1 kinase can directly phosphorylate Ajuba, we performed in vitro kinase assays with His-tagged Ajuba proteins as substrates. Fig. 1-2A shows that Taxol-treated mitotic lysates robustly phosphorylated Ajuba and that addition of RO3306 or Purvalanol A greatly reduced phosphorylation of His-Ajuba (Fig. 1-2A). As expected, purified CDK1-cyclin B kinase complex phosphorylated His-Ajuba proteins in vitro (Fig. 1-2B). These results indicate that CDK1 directly phosphorylates Ajuba in vitro.

1.3.4. CDK1-Cyclin B Complex Phosphorylates Ajuba at Ser ^{119} in Vitro and in Cells

CDK1 phosphorylates substrates at a minimal proline-directed consensus sequence [40]. Ajuba contains a total of 6 (S/T) P motifs (Thr30, Ser119, Ser137, Ser175, Ser196, and Ser237). Interestingly, two of them (Ser119 and Ser175) were identified as mitotic phosphorylation sites by previous phospho-proteomic studies [41] and mutating these two sites to alanine abolished the 32P incorporation in His-Ajuba, suggesting that Ser119 and Ser175 are the main CDK1 sites in Ajuba in vitro (Fig. 1-2C). Ser119 and Ser175 are

highly conserved in vertebrates (Fig. 1-2D). Therefore, these two sites were chosen for further study.

We have generated phospho-specific antibodies against Ser119 and Ser175. In vitro kinase assays demonstrated that CDK1 readily phosphorylates Ajuba at Ser119 (Fig. 1-2E). Very weak signal was detected when the phospho-Ser175 antibody was used under these conditions (data not shown). Addition of RO3306 or mutating Ser119 to alanine abolished the phosphorylation (Fig. 1-2E). These data suggest that CDK1 phosphorylates Ajuba at Ser119 in vitro. Taxol treatment significantly increased the phosphorylation of Ser119 on endogenous Ajuba (Fig. 1-2F). Using inhibitors for CDK1 kinase, we demonstrated that phosphorylation of Ajuba Ser119 is CDK1 kinase dependent (Fig. 1-2F). The signal of Ajuba Ser119 during Taxol treatment was significantly reduced in Ajuba knockdown cells, confirming the specificity of the phospho-Ser119 antibody (Fig. 1-2G). Taxol treatment also increased the phosphorylation of Ser119 on transfected Ajuba, and the signal was abolished by mutating Ser119 to alanine (Fig. 1-2H), suggesting that these antibodies specifically recognize phosphorylated Ajuba. Taken together, these observations indicate that Ajuba is phosphorylated at Ser119 by CDK1 in cells during antimitotic drug-induced G2/M arrest.

1.3.5. CDK1/Cyclin B Mediates Ajuba Phosphorylation at Ser^{119} and Ser^{175} in Cells

We next performed immunofluorescence microscopy with these phospho-specific antibodies. Both antibodies against Ser119 and Ser175 detected strong signals in Nocodazole-arrested prometaphase cells (Fig. 1-3, A-C, white arrows). The sign was always very low or not detectable in interphase cells (Fig. 1-3, A-C, yellow arrows). The specificity of the antibodies was further confirmed by peptide blocking assays. Phospho-

peptide, but not control non-phosphopeptide, incubation completely blocked the signal, suggesting that these antibodies specifically recognize Ajuba only when it is phosphorylated (Fig. 1-3, A and B). Again, addition of RO3306 or Purvalanol A largely diminished the signals detected by p-Ajuba Ser119 and Ser175 antibodies in Nocodazole-treated prometaphase cells, further indicating that the phosphorylation is CDK1 dependent (Fig. 1-3, A and B, low panels).

1.3.6. Ajuba Phosphorylation Occurs during Normal Mitosis

To determine whether phosphorylation of Ajuba occurs during normal mitosis, we collected samples from a double thymidine block and release [38] and performed immunofluorescence staining on cells in different cell-cycle phases. Consistent with Fig. 1-3, a very weak signal was detected in interphase or cytokinesis cells (Fig. 1-4, A and B). The p-Ajuba Ser^{119} signal was increased in prophase and the strongest signal was detected in prometaphase/metaphase cells. The signal was then again weakened during telophase (Fig. 1-4, A and B). Similar staining patterns were observed with p-Ajuba Ser^{175} antibody (Fig. 1-4, C and D). After being released from the double thymidine block, cells enter into mitosis at 10-12 h revealed by increased Phospho-Histone H3 (Ser^{10}) and the p-Ajuba Ser^{119} signal was also increased in these cells (Fig. 1-4E). These results indicate that Ajuba phosphorylation occurs dynamically during normal mitosis.

1.3.7. Mitotic Phosphorylation of Ajuba Impacts Cell Cycle Regulators without Affecting YAP Activity

Ajuba was shown to affect the Hippo-YAP signaling activity through interacting with Lats1/2 kinase [17-19]. We confirmed that the association between Ajuba and Lats2 was readily detected (Fig. 1-5A). Non-phosphorylatable (Ajuba-2A, S119A/S175A) or a

phosphomimetic (Ajuba-2D, S119D/S175D) mutant has similar binding affinity with Lats2 as wild type Ajuba (Fig. 1-5A), suggesting that Ajuba phosphorylation does not impact its association with Lats2. YAP Ser^{127} phosphorylation, Lats activity (revealed by phospho-Ser^{909}), and the levels of YAP and Lats proteins were not significantly altered when Ajuba was overexpressed (in HPNE, immortalized pancreatic epithelial cells) or knocked down (in RCA colon cancer cells) (Fig. 1-5B). Epithelial-mesenchymal transition is a critical process during development, wound healing, and stem cell behavior, and contributes pathologically to cancer progression and metastasis [42]. Several members of the Hippo-YAP signaling regulate epithelial-mesenchymal transition. However, manipulation of Ajuba expression failed to influence the expression of the epithelial-mesenchymal transition markers (Fig. 1-5B). In line with these observations, the targets expression of YAP was not affected by Ajuba expression in HPNE and RCA cells (Fig. 1-5, C and D). These results suggest that mitotic phosphorylation of Ajuba does not affect YAP activity and that Ajuba influences Hippo-YAP activity in a context-dependent manner.

We further determined whether Ajuba/mitotic phosphorylation affects cell cycle regulators. Interestingly, the expression of several genes (including CDC25C, BUB1 and phosphorylated Wee1) was increased upon Ajuba knockdown in RCA cells (Fig.1-5E). Moreover, re-expression of wild type Ajuba, but not the Ajuba-2A mutant, rescued the phenotype (Fig. 1-5E). These observations suggest that Ajuba and its phosphorylation may have a role in cell cycle progression through regulation of the expression of cell cycle regulators.

1.3.8. Mitotic Phosphorylation of Ajuba Is Required for Cell Proliferation and Anchorage-independent Growth

Next we asked what the biological significance of mitotic phosphorylation of Ajuba is. To address this question, we first established HPNE cell lines stably expressing Ajuba or non-phosphorylatable Ajuba mutant (Ajuba-2A) (Fig. 1-6A). Interestingly, overexpression of Ajuba significantly increased cell proliferation when compared with control cells. However, cells expressing Ajuba-2A proliferated at a rate similar to that of control cells, suggesting that mitotic phosphorylation of Ajuba promotes cell proliferation (Fig. 1-6B). Ectopic expression of Ajuba (wild type or 2A or 2D) was not sufficient to stimulate anchorage-independent growth in soft agar in HPNE cells (data not shown). We further determined the impact of mitotic phosphorylation of Ajuba in cancer cells. We established RCA cell lines in which the endogenous Ajuba was replaced with shRNA-resistant Ajuba or Ajuba-2A in a Tet-inducible manner (Fig. 1-6C). Without doxycycline induction, these cell lines express similar levels of endogenous Ajuba proteins (Fig. 1-6C, left 4 lanes) and no proliferation or other differences were detected among these cells. Addition of doxycycline to the cell culture medium induced endogenous Ajuba knockdown and expression of shRNA-resistant Ajuba or its non-phosphorylatable mutant (Fig. 1-6C, right 4 lanes). Consistent with the Ajuba overexpression results in HPNE cells, knockdown of Ajuba in RCA cells decreased proliferation, and importantly, expression of wild type Ajuba, but not the non-phosphorylatable mutant Ajuba-2A, completely rescued the cell proliferation defects (Fig. 1-6D). Furthermore, Ajuba knockdown also significantly decreased anchorage-independent growth in soft agar, and again, re-expression of Ajuba-2A failed to rescue the defects, whereas wild type Ajuba did (Fig. 1-6, E and F). These data suggest that mitotic phosphorylation is essential for Ajuba to promote cell proliferation and anchorage-independent growth.

1.3.9. Mitotic Phosphorylation of Ajuba Is Required for Tumorigenesis

We next evaluated the influence of Ajuba and its mitotic phosphorylation on tumor growth in animals. RCA cells in which the endogenous Ajuba was replaced with shRNA-resistant wild type Ajuba or Ajuba-2A (Fig. 1-6C) were subcutaneously inoculated into immunodeficient mice. Interestingly, tumors from mice harboring Ajuba-2A-expressing cells tended to be smaller when compared with those from mice injected with Ajuba-expressing cells (Fig. 1-7A and B). Histopathological examination revealed no significant differences among these tumors (Fig. 1-7C). Consistent with Fig. 1-5E, CDC25C expression was higher in Ajuba-2A-expressing tumors than Ajuba-WT tumors (Fig. 1-7C). Western blotting analysis confirmed the phosphorylation status of Ser^{119}, and verified that Ajuba (wild type or 2A) expression levels were similar in most of these tumors (Fig. 1-7D). These results support the hypothesis that mitotic phosphorylation is essential for Ajuba promoted tumor growth in vivo.

A previous report showed that Ajuba was up-regulated in colon cancer cell lines and tumors [22]. We further analyzed the expression of Ajuba in published data and confirmed that the mRNA levels of Ajuba were significantly increased in colon tumors compared with normal colon (Fig. 1-7, E–H). Together, these observations indicate that Ajuba functions as a tumor-promoting regulator in colon cancer in a mitotic phosphorylation-dependent manner.

1.4. Discussion

Ajuba family proteins (Ajuba, LIMD1, and WTIP) play roles in various cellular processes, and one of the most studied areas is the role of Ajuba protein in mitosis. Ajuba is required for mitotic entry in coordination with Aurora-A kinase and is co-localized at centrosomes with Aurora-A, CDK1/cyclin B [27], and Lats2 [28] during G2/mitosis. Interestingly, Ajuba protein became phosphorylated in mitotic cells; however, there are differing reports regarding the kinase that contributes to this mitotic phosphorylation. Hirota et al. [27] showed that Aurora-A directly phosphorylated Ajuba in vitro but did not investigate whether Ajuba phosphorylation is Aurora-A dependent in cells. Another report suggested that Lats2 contributed to Ajuba phosphorylation during mitosis [28]. The current study provided evidence that CDK1 is the major kinase responsible for Ajuba phosphorylation and that CDK1 phosphorylates Ajuba in vitro and in cells during mitosis, adding a new layer of regulation for Ajuba during mitosis. Our data do not exclude the possibility that Aurora-A and Lats2 kinases can phosphorylate Ajuba in cells as well. Future studies are needed to further define the mitotic phosphorylation (phosphorylation sites and their biological function) of Ajuba by Aurora-A and/or Lats2. Of note, several large scale proteomic studies have identified Ser^{119} and Ser^{175} as mitotic phosphorylation sites and both sites fit the CDK1-phosphorylation consensus sequence [41].

In Drosophila, Djub promotes cell proliferation and inhibits apoptosis by regulating Hippo-Yki activity [17]. Consistent with these observations, our data further confirm that Ajuba is a positive regulator for cell proliferation and anchorage-independent growth in pancreatic and colon cancer cells (Fig. 1-6). Furthermore, Ajuba also promotes migration and invasion in colon cancer cells [22]. Interestingly, whereas these studies clearly showed that Ajuba promotes cell proliferation, Ajuba was shown to suppress malignant mesothelioma cell proliferation [23], suggesting a cell type-specific role of Ajuba in cancer

cells. In line with a role of Ajuba in cancer, recent large scale genomic studies found that the Ajuba gene is mutated in 7% of esophageal squamous cell carcinomas [24, 25] and Ajuba is overexpressed in colon cancer patients [22]. Our current study further demonstrates that mitotic phosphorylation of Ajuba by CDK1 is critical for its biological function, suggesting that there is a link between the role of Ajuba in cancer and its mitotic regulation and that Ajuba may exert its role in cancer through deregulation in mitosis. Together, these studies suggest that Ajuba may play a role in tumorigenesis, although further confirmation will require genetic animal models. Ajuba is not essential for embryo development and Ajuba knock-out mice have no obvious phenotypes [43]. These observations suggest that Ajuba may function as a fine regulator in tumorigenesis and needs an additional allele product to promote/inhibit tumor cell growth. However, knock-out of the Ajuba allele has not been combined with any other oncogenes or tumor suppressors including ones in the Hippo-YAP pathway. In addition, since there is functional redundancy and overlapping expression within the Ajuba family proteins [21], clearly defining the biological role of Ajuba in tumorigenesis may be even more challenging.

Mitotic aberrations cause genomic/chromosome instability, which is characteristic of human malignancy [44]. Several reports showed that the Hippo pathway plays important roles in maintaining normal mitosis and suggest a mechanism through which the Hippo tumor suppressor pathway exerts its function. For example, loss of core tumor suppressors in the Hippo pathway (including Lats2, MST1/2, Mob1, and WW45) leads to severe defects in multiple mitotic processes [45-47]. Accordingly, we recently reported that overexpression of active YAP [12, 13] or TAZ [15] is sufficient to trigger mitotic defects, including centrosome amplification, spindle disorganization, chromosome misalignment, and subsequent aneuploidy. Interestingly, we also found that several Hippo core members

(Lats1, Lats2, and MST2) (Fig. 1-1) or their upstream regulator (KIBRA) [30, 31] or downstream effectors (YAP and TAZ) [12, 13, 15] are phosphorylated during mitosis. Importantly, mitotic phosphorylation is critical for their oncogenic or tumor suppressive functions [12, 13, 15]. These observations suggest that in addition to their expression levels, the phosphorylation status of these proteins must also be finely controlled, adding another layer of regulation for Hippo-YAP activity during tumorigenesis. Such studies may provide additional insights into the underlying mechanisms of Hippo-YAP signaling in cancer. Thus, we extended our studies to other Hippo regulators and we found that the Ajuba/Zyxin family proteins (Ajuba, LIMD1, and Zyxin) are also phosphorylated during antimitotic drug-induced mitotic arrest (Fig. 1-1). Zxyin was previously shown to be phosphorylated and played a role in mitosis; however, the phosphorylation sites, corresponding kinase, and their functional significance remain elusive [48]. Although these proteins are structurally and functionally related, sites analogous to Ajuba Ser^{119} and Ser^{175} do not exist on LIMD1 and Zyxin. Additionally, the role of LIMD1 and its regulation in mitosis also remain to be defined. Addressing these questions will not only help understand the cellular function of these proteins in mitosis, but also provide insights into their biological significance and underlying mechanisms in cancer development.

Figure 1-1. CDK1-dependent phosphorylation of Ajuba during G2/M arrest.

(A) HeLa cells were treated with DMSO, Taxol (100 nM for 16 h), or Nocodazole (Noco, 100 ng/ml for 16h). Total cell lysates were probed with the indicated antibodies against Hippo components on Phos-tag SDS-polyacrylamide gels (see “Experimental Procedures”). O and * mark the non-phosphorylated and phosphorylated proteins, respectively. (B) HeLa cells were treated with Taxol as indicated and cell lysates were further treated with (+) or without (-) λ-phosphatase (ppase). Total cell lysates were probed with anti-Ajuba antibody. (C) HeLa cells were treated with Taxol together with or without various kinase inhibitors as indicated. VX680 (2 μM), MK5108 (10 μM), ZM447439(1 μM), RO3306(5 μM), Roscovitine (30 μM), Purvalanol A (10 μM), and BI2536 (100 nM) were used. Inhibitors were added (with MG132 to prevent cyclin B from degradation and cells from exiting from mitosis) 1 - 2 h before harvesting the cells. Total cell lysates were subjected to Western blotting with the indicated antibodies.

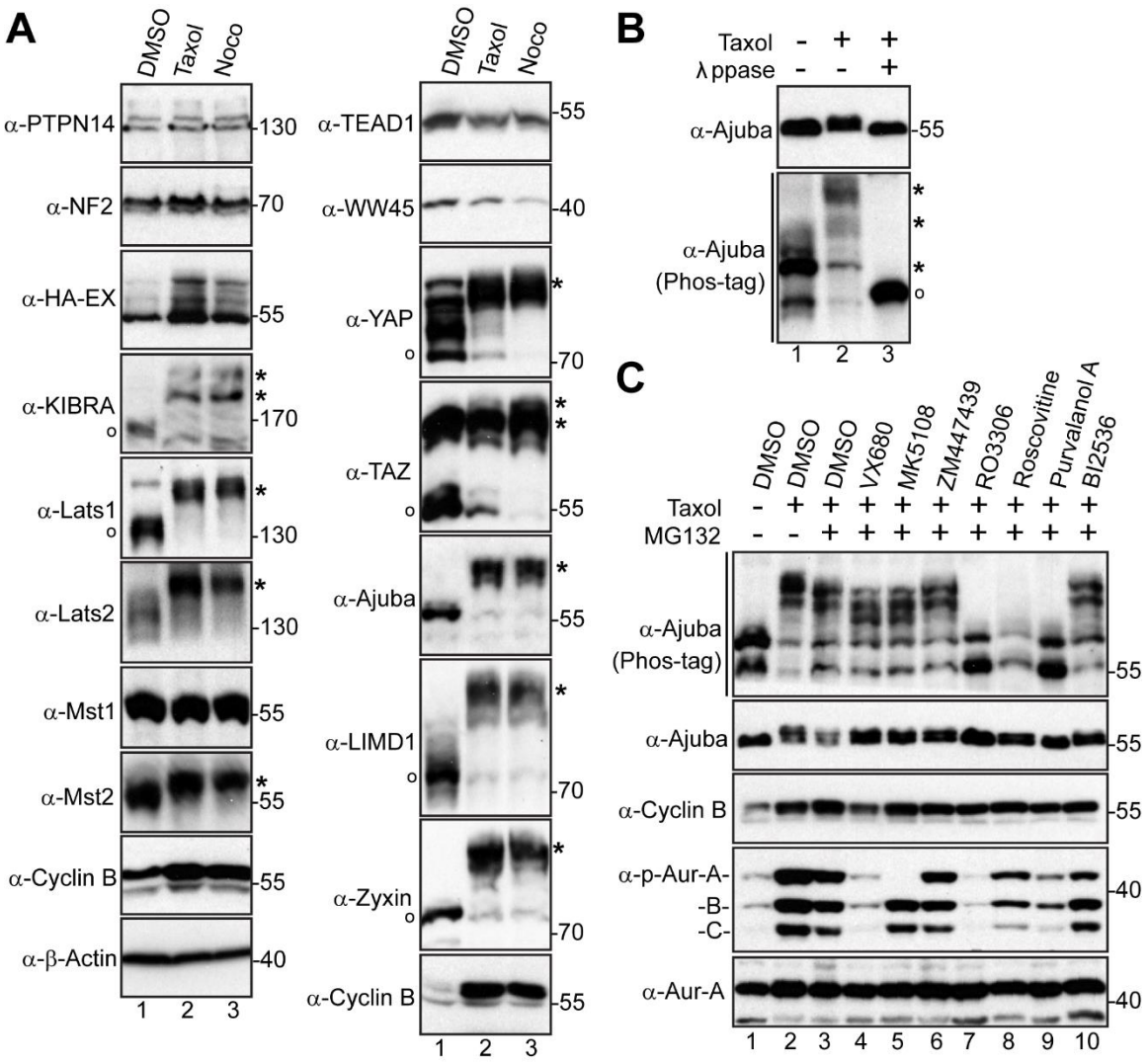
A
DMSO
Taxol
Noco
α-PTPN14
130
α-NF2
70
α-HA-EX
55
α-KIBRA
170
α-Lats1
130
α-Lats2
130
α-Mst1
55
α-Mst2
55
α-Cyclin B
55
α-β-Actin
40
1 2 3
α-TEAD1
55
α-WW45
40
α-YAP
70
α-TAZ
55
α-Ajuba
55
α-LIMD1
70
α-Zyxin
70
α-Cyclin B
55
1 2 3
B
Taxol - + +
λppase - - +
α-Ajuba
55
α-Ajuba
(Phos-tag)
1 2 3
C
DMSO
DMSO
DMSO
VX680
MK5108
ZM447439
RO3306
Roscovitine
Purvalanol A
BI2536
Taxol - + + + + + + + + +
MG132 - - + + + + + + + +
α-Ajuba
(Phos-tag)
55
α-Ajuba
55
α-Cyclin B
55
α-p-Aur-A-
-B-
-C-
40
α-Aur-A
40
1 2 3 4 5 6 7 8 9 10

Figure 1-2. Ajuba is phosphorylated by CDK1 in vitro and in cells

(A) In vitro kinase assays using HeLa cell lysates to phosphorylate recombinant His-Ajuba. Asy,asynchronized; Tax, Taxol-treated. Total cell lysates were probed with cyclin B and β-actin antibodies. RO3306 (5 μM) or PurvalanolA (10 μM) was used to inhibit CDK1 kinase activity. (B) In vitro kinase assays with purified CDK1/cyclin B complex. RO3306 (5 μM) was used to inhibit CDK1 kinase activity. (C) In vitro kinase assays with purified CDK1/cyclin B complex. 2A, S119A/S175A. (D) Conservation of the mitotic phosphorylation sites of Ajuba. (E) In vitro kinase assays were done as in B except anti-phospho-Ajuba Ser^{119} antibodies were used. (F) HeLa cells were treated with Taxol together with or without various kinase inhibitors as indicated. Inhibitors were added (with MG132 to prevent cyclin B from degradation and cells from exiting from mitosis) 1h before harvesting the cells. Total cell lysates were subjected to Western blotting with the indicated antibodies. (G) RKO colon cancer cells expressing Tet-control shRNA or Tet-shRNA Ajuba (#1 and #2) in the presence of doxycycline (1μg/ml for 2 days) were treated with (+) or without (-) Taxol and total cell lysates were subjected to Western blotting with the indicated antibodies. (H) HEK293T cells were transfected with GFP-Ajuba or GFP-Ajuba mutants. At 32h post-transfection, the cells were treated with Taxol for 16 h. The immunoprecipitates (with GFP antibodies) were probed with anti-phospho-Ajuba and subsequent anti-GFP antibodies. Total cell lysates before immunoprecipitation were also included (cyclin B and β-actin).

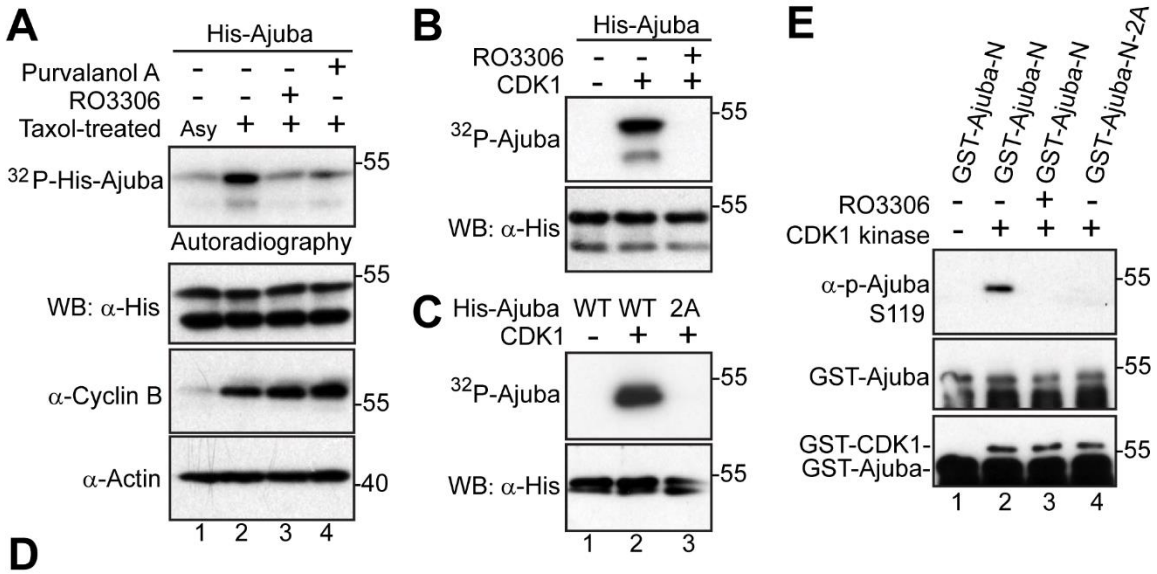

D

Xenopus laevis (frog)	214-GQYEGGVL**S**PRSSYASTT	SMGYDQRHI**S**PRSSTAS-278
Danio rerio (zebrafish)	270-SLQESVLA**S**PRSSFASST	SLGYDNRH-**T**PGPAQQL-328
Mus musculus (mouse)	121-LEPTAPAL**S**PRSSFASSS	SMGYDQRHG**S**PLPAGPC-192
Homo sapiens (human)	111-LEPTAPAL**S**PRSSFASSS	SMGYDQRHG**S**PLPAGPC-182
	S119	S175

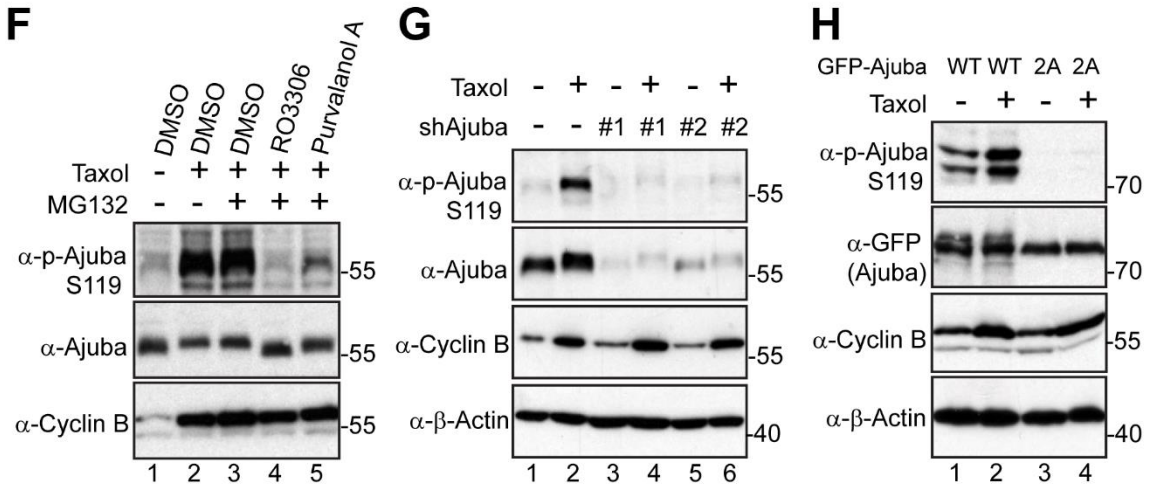

Figure 1-3. CDK1 mediates the phosphorylation of Ajuba at Ser^{119} and Ser^{175} during G2/M phase arrest.

(A) HeLa cells were treated with Nocodazole for 8h and then fixed. Before the cells were stained with phospho-specific antibody against Ser^{119} of Ajuba, the cells were pre-incubated with PBS (no peptide control), or non-phosphorylated (control) peptide, or the phosphorylated peptide used for immunizing rabbits. CDK1 inhibitors RO3306 (5μM) or Purvalanol A (10μM) together with MG132 (25 μM) were added 2 h before the cells were fixed (bottom two rows). (B) Experiments were done similarly as in A with phospho-specific antibody against Ser^{175} of Ajuba. (C) HeLa cells were treated and stained with phospho-specific antibodies as in A and B. An X63 oil objective lens was used to view fewer cells in a field. P-H3 S^{10} was used as a mitotic marker. White and yellow arrows mark some of the prometaphase cells and the interphase cells, respectively.

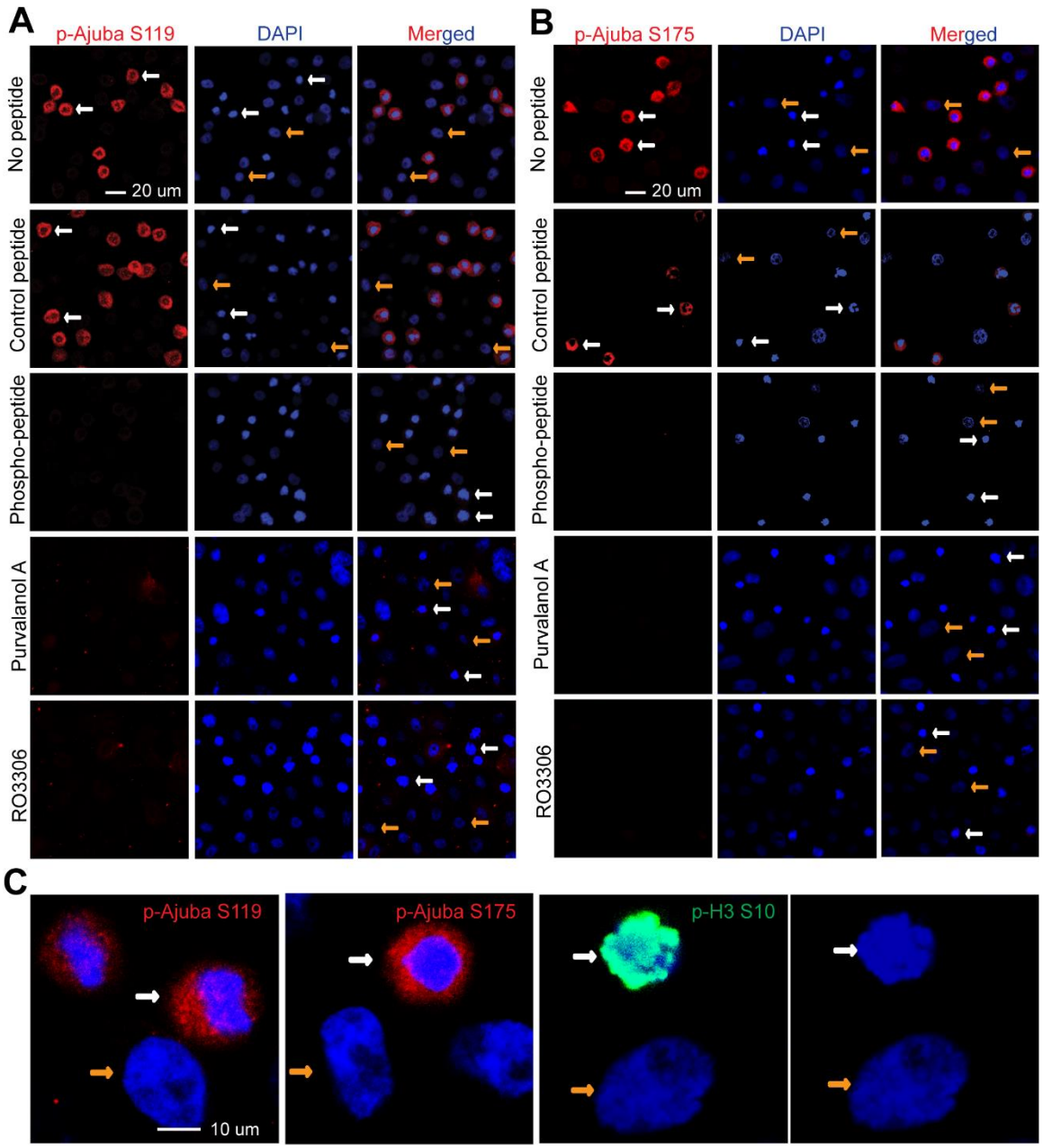
A
p-Ajuba S119
DAPI
Merged
No peptide
Control peptide
Phospho-peptide
Purvalanol A
RO3306
20 um
B
p-Ajuba S175
DAPI
Merged
No peptide
Control peptide
Phospho-peptide
Purvalanol A
RO3306
20 um
C
p-Ajuba S119
p-Ajuba S175
p-H3 S10
10 um

Figure 1-4. Ajuba is phosphorylated at Ser^{119} and Ser^{175} during unperturbed mitosis. (A-B) HeLa cells were synchronized by a double thymidine (DT) block and release method. Cells were stained with antibodies against p-Ajuba Ser119 or β-tubulin, or with DAPI. An X40 objective lens was used to view various phases of the cells in a field (B). (C-D) The experiments were done similarly as in A and B with p-Ajuba Ser175 antibodies. White and yellow arrows (in panels B and D) mark the metaphase and interphase cells, respectively. (E) HeLa cells were synchronized by a double thymidine block and release method. Total cell lysates were harvested at the indicated time points and subjected to Western blotting analysis.

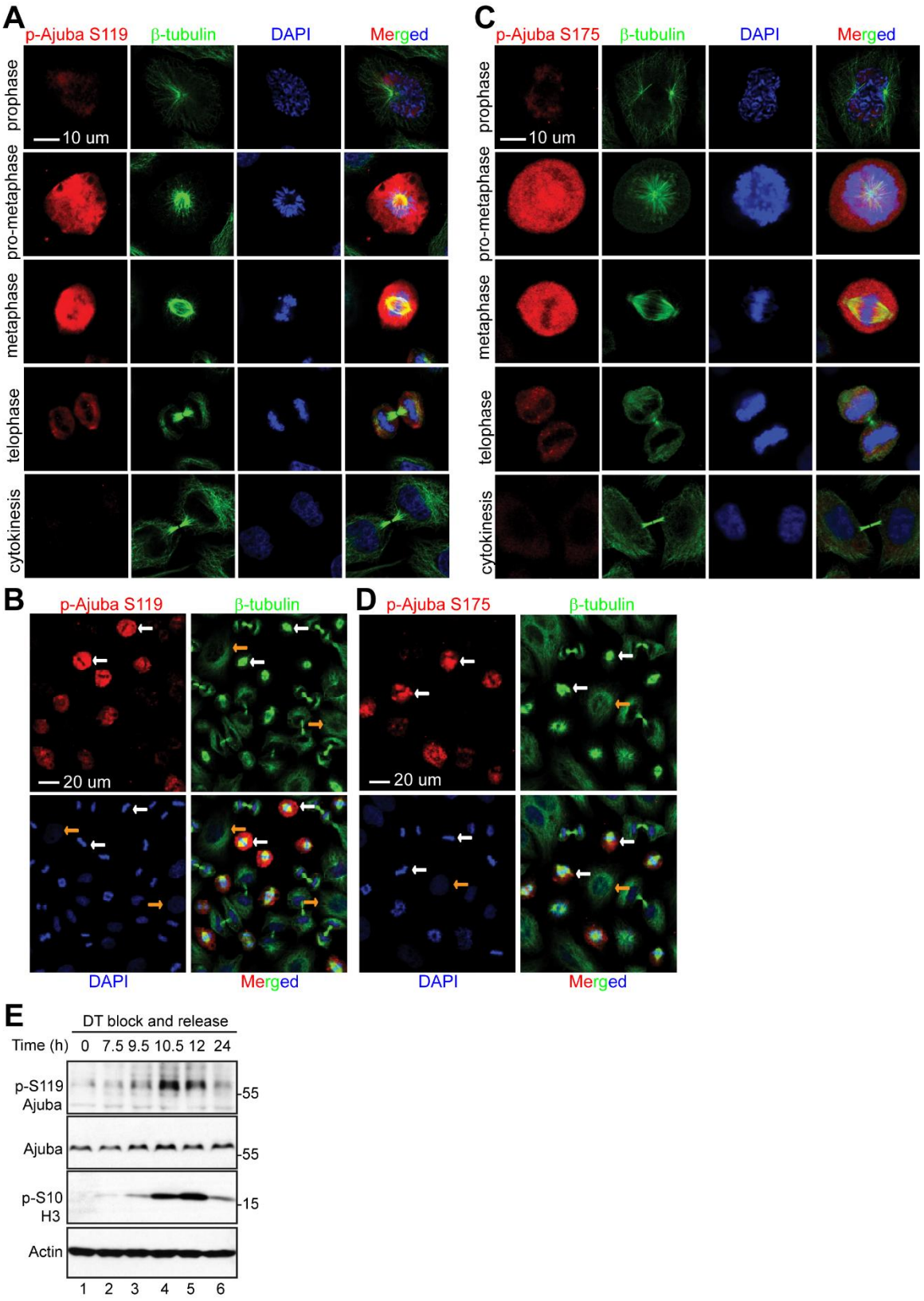
A
p-Ajuba S119
β-tubulin
DAPI
Merged
prophase
pro-metaphase
metaphase
telophase
cytokinesis
10 um
C
p-Ajuba S175
β-tubulin
DAPI
Merged
B
p-Ajuba S119
β-tubulin
20 um
DAPI
Merged
D
p-Ajuba S175
β-tubulin
20 um
DAPI
Merged
E
DT block and release
Time (h) 0 7.5 9.5 10.5 12 24
p-S119 Ajuba
Ajuba
p-S10 H3
Actin
55
55
15
1 2 3 4 5 6

Figure 1-5. Mitotic phosphorylation controls the expression of cell cycle regulators, but does not affect the Hippo-YAP activity.

(A) HEK293T cells were transfected with various DNA plasmids as indicated. The immunoprecipitates (with Myc antibodies) were probed with anti-Ajuba and subsequent anti-Myc antibodies. Total cell lysates before immunoprecipitation were also included (Input). (B) Total cell lysates from various HPNE and RCA cell lines as indicated were probed with the indicated antibodies. HPNE cells were stably transduced with vector, Ajuba, Ajuba-2A, or Ajuba-2D. Tet-On-inducible Ajuba-knockdown cell lines expressing shRNA-resistant Ajuba or Ajuba-2A in RCA colon cancer cells were also established (see “Experimental Procedures“). 2A, S119A/S175A; 2D, S119D/S175D. (C-D) Quantitative RT-PCR for CTGF and Cyr61 in cell lines established in B. (E) Total cell lysates were harvested from RCA cell lines established in B and were subjected to Western blotting analysis with various cell cycle regulators.

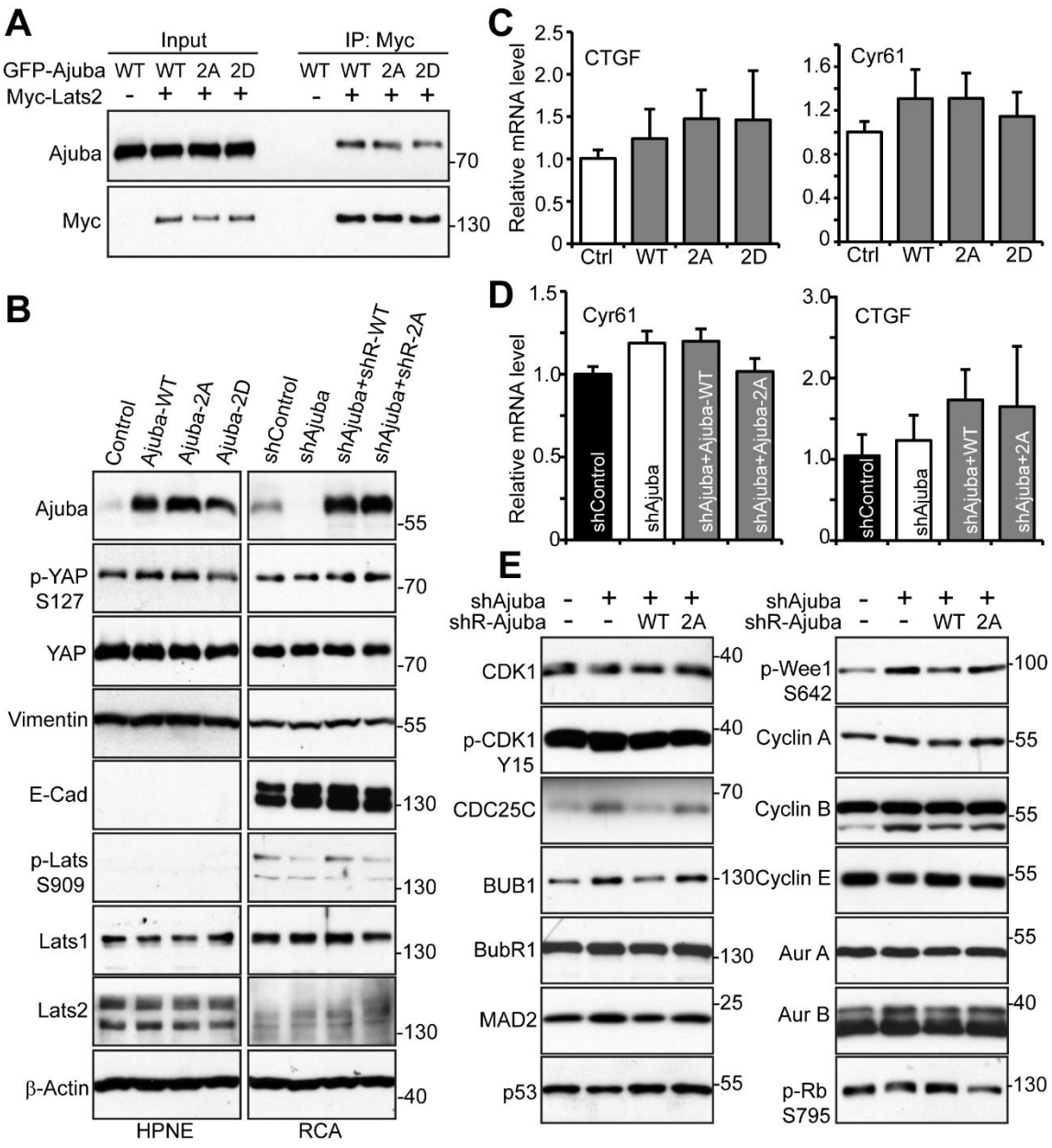
A
Input
IP: Myc
GFP-Ajuba WT WT 2A 2D WT WT 2A 2D
Myc-Lats2 - + + + - + + +
Ajuba
Myc
70
130
B
Control
Ajuba-WT
Ajuba-2A
Ajuba-2D
shControl
shAjuba
shAjuba+shR-WT
shAjuba+shR-2A
Ajuba
p-YAP S127
YAP
Vimentin
E-Cad
p-Lats S909
Lats1
Lats2
β-Actin
55
70
70
55
130
130
130
130
40
HPNE
RCA
C
CTGF
Cyr61
Relative mRNA level
Ctrl WT 2A 2D
D
Cyr61
CTGF
Relative mRNA level
shControl
shAjuba
shAjuba+Ajuba-WT
shAjuba+Ajuba-2A
shAjuba+WT
shAjuba+2A
E
shAjuba - + + +
shR-Ajuba - - WT 2A
CDK1
p-CDK1 Y15
CDC25C
BUB1
BubR1
MAD2
p53
40
40
70
130
130
25
55
p-Wee1 S642
Cyclin A
Cyclin B
Cyclin E
Aur A
Aur B
p-Rb S795
100
55
55
55
55
40
130

Figure 1-6. Mitotic phosphorylation of Ajuba is required for cell proliferation and anchorage-independent growth.

(A) HPNE cells stably expressing vector, Ajuba, or Ajuba-2A were established, and expression of Ajuba and Ajunba-2A were confirmed by Western blotting. 2A, S119A/S175 A. (B) Cell proliferation assays with transduced HPNE cells established in A. Data were expressed as the mean ± S.D. of three independent experiments. ***, $p<0.001$;*, $p<0.05$ (Ajuba-WT versus Ajuba-2A) (*t* test). (C) Establishment of Tet-On-inducible Ajuba-knockdown cell lines expressing shRNA-resistant Ajuba or Ajuba-2A in RCA colon cancer cells (see “Materials and Methods“). Cells were kept on Tet-approved FBS and doxycycline was added (1 μg/ml) to the cells 2 days prior to the experiments. (D) Cell proliferation assays in RCA cells established in C in the presence of doxycycline (DOX). Data were expressed as the mean ± S.D. of three independent experiments. Red asterisks mark the comparisons between shControl and shAjuba. Green asterisks indicate the comparisons between Tet-Ajuba-WT and Tet-Ajuba-2A. ***, $p<0.001$;**, $p<0.01$;*, $p<0.05$ (*t* test). (E-F), colony assays in soft agar to assess anchorage-independent growth of RCA cells established in C in the presence of doxycycline. Data were expressed as the mean ± S.D. of three repeats (E) and representative images were shown (F). ***, $p<0.001$;**, $p<0.01$ (*t* test).

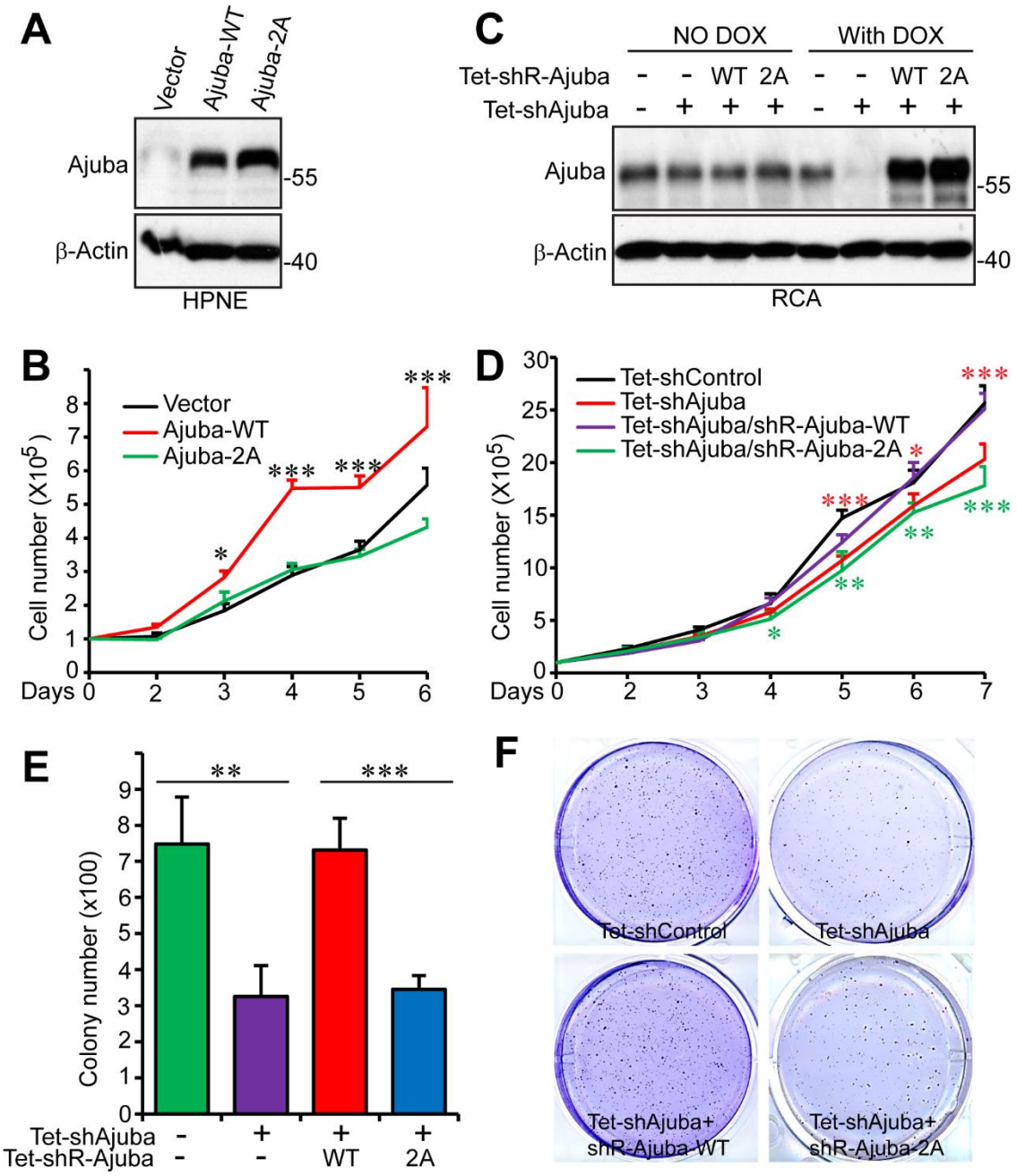
A
Vector
Ajuba-WT
Ajuba-2A
Ajuba
-55
β-Actin
-40
HPNE
C
NO DOX
With DOX
Tet-shR-Ajuba - - WT 2A - - WT 2A
Tet-shAjuba - + + + - + + +
Ajuba
-55
β-Actin
-40
RCA
B
Vector
Ajuba-WT
Ajuba-2A
Cell number (X10^5)
Days
D
Tet-shControl
Tet-shAjuba
Tet-shAjuba/shR-Ajuba-WT
Tet-shAjuba/shR-Ajuba-2A
Cell number (X10^5)
Days
E
Colony number (x100)
Tet-shAjuba - + + +
Tet-shR-Ajuba - - WT 2A
F
Tet-shControl
Tet-shAjuba
Tet-shAjuba+ shR-Ajuba-WT
Tet-shAjuba+ shR-Ajuba-2A

Figure 1-7. Ajuba phosphorylation is essential for tumorigenesis in mice.

(A) Tumor growth curve. RCA cells expressing Tet-shRNA Ajuba and shRNA-resistant wild type Ajuba or Ajuba-2A were subcutaneously inoculated into athymic nude mice (Ajuba-WT on the left flank and Ajuba-2A on the right flank) and the mice were kept on doxycycline (0.5mg/ml) in their drinking water throughout the experiment. Two of ten mice did not form visible tumors (both left and right sides) and were excluded from the analysis. Therefore, the tumor volume at each point was the average of 8 tumors. The p values are also shown. **, $p<0.01$;*, $p<0.05$ (*t* test). (B) The largest four tumors in each group were excised and photographed at the endpoint. C, hematoxylin and eosin (H&E) and CDC25C IHC staining in tumors shown in B. (D) Western blotting analysis with tumor samples from B. (E-H) The mRNA levels of Ajuba in normal colon and colon tumors from public data sets. Data were mined from Oncomine.org. The original studies were as follows: Refs. [49](E), [50](F), [51](G), and [52] (H).Tumors, colorectal carcinoma; CA, colorectal adenocarcinoma.

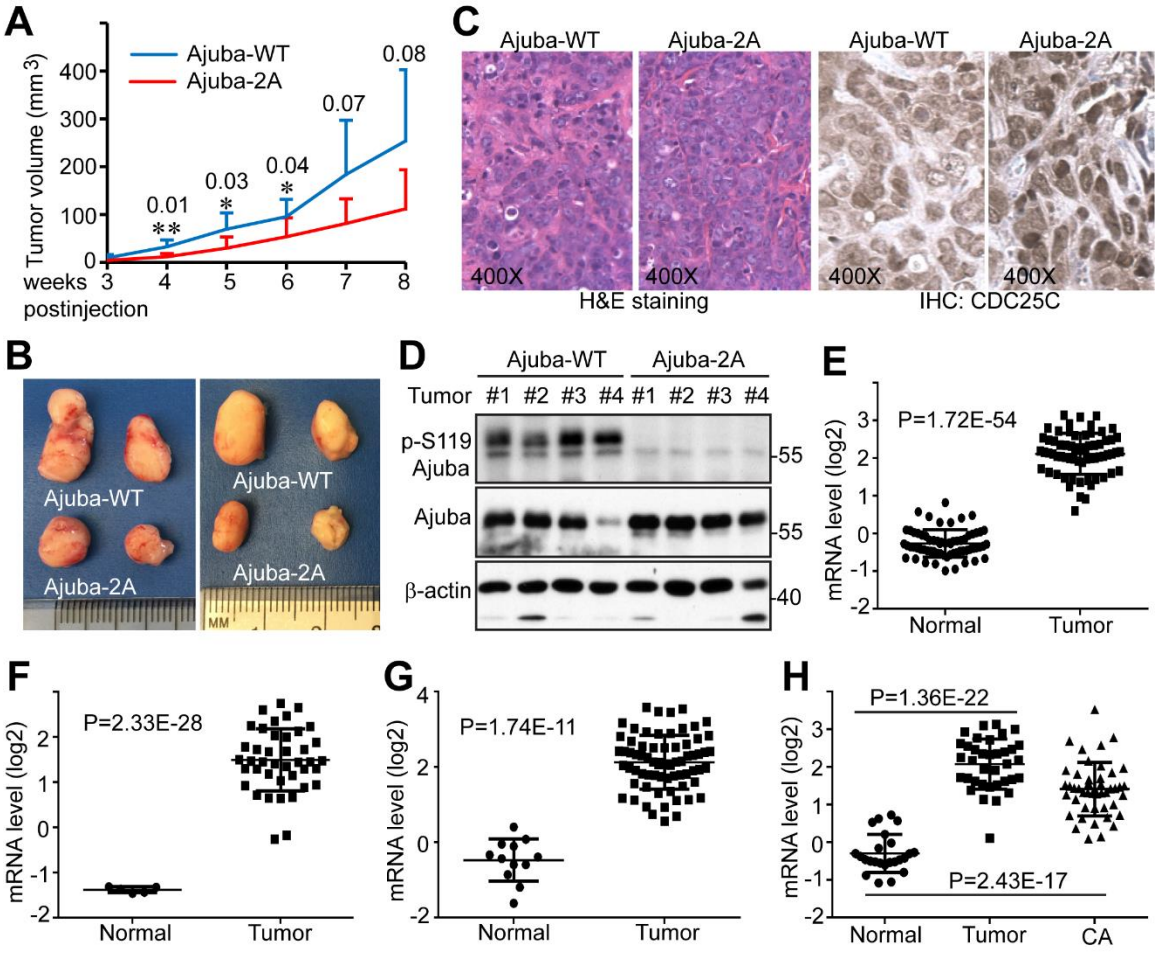
A
Tumor volume (mm3)
Ajuba-WT
Ajuba-2A
0.01
0.03
0.04
0.07
0.08
weeks postinjection
C
Ajuba-WT
Ajuba-2A
400X
H&E staining
IHC: CDC25C
B
Ajuba-WT
Ajuba-2A
D
Tumor #1 #2 #3 #4 #1 #2 #3 #4
p-S119 Ajuba
Ajuba
β-actin
55
40
E
P=1.72E-54
mRNA level (log2)
Normal
Tumor
F
P=2.33E-28
G
P=1.74E-11
H
P=1.36E-22
P=2.43E-17
CA

CHAPTER 2: MST2 PHOSPHORYLATION AT SERINE 385 IN MITOSIS INHIBITS ITS TUMOR SUPPRESSING ACTIVITY*

* The material presented in this chapter was previously published: Chen *et al. Cell Signal* 2016; 28(12): 1826-1832.

ABSTRACT

Mammalian sterile 20-like kinase 1/2 (MST1/2) are core tumor suppressors in the Hippo signaling pathway. MST1/2 have been shown to regulate mitotic progression. Here, we report a novel mechanism for phospho-regulation of MST2 in mitosis and its biological significance in cancer. We found that the mitotic kinase cyclin-dependent kinase 1 (CDK1) phosphorylates MST2 *in vitro* and *in vivo* at serine 385 during antimitotic drug-induced G2/M phase arrest. This phosphorylation occurs transiently during unperturbed mitosis. Mitotic phosphorylation of MST2 does not affect its kinase activity or Hippo-YAP signaling. We further showed that mitotic phosphorylation-deficient mutant MST2-S385A possesses higher activity in suppressing cell proliferation and anchorage-independent growth *in vitro* and tumorigenesis *in vivo*. Together, our findings reveal a novel layer of regulation for MST2 in mitosis and its role in tumorigenesis.

2.1. Introduction

Mammalian sterile 20-like kinase 1/2 (MST1/2) are protein kinases that belong to the serine/threonine kinase family (MST1 and MST2 are also called STK4 and STK3, respectively). MST1/2 are the core components of the Hippo pathway and transduce their kinase activity mainly through directly phosphorylating large tumor suppressor 1/2 (LATS1/2) [2, 5]. Once phosphorylated and activated, LATS1/2 subsequently phosphorylate and inhibit the downstream effectors Yes-associated protein (YAP) and transcriptional co-activator with PDZ binding domain (TAZ) [2, 5, 6, 8]. Neither MST1 nor MST2 alone is required for embryonic development, but double knock out of MST1/2 mice exhibit early embryonic lethality, suggesting a redundant and overlapping function between MST1 and MST2 [53]. Recent studies using conditional MST1/2 knockout animal models demonstrated that MST1/2 function as tumor suppressors [53-56]. In addition to their role as tumor suppressors in the Hippo signaling pathway, MST1/2 also phosphorylate several other proteins to exercise their functions in various cellular processes, mainly in cell proliferation and apoptosis [57].

Mitotic aberration-induced genomic or chromosome instability is characteristic of human malignancy [44, 58]. Several recent studies have shown that MST1/2 are important regulators for the mitotic machinery. MST1 phosphorylates and inhibits Aurora B kinase activity and is required for accurate kinetochore-microtubule attachment [59]. PLK1 (Polo-like kinase 1) directly phosphorylates MST2 (possibly MST1 as well) in mitosis and this phosphorylation allows Nek2A kinase activity to promote centrosome disjunction [60]. These studies suggest that MST1/2 function as tumor suppressors through dysregulation of mitosis.

We have recently shown that several upstream regulators (KIBRA and Ajuba) [30, 31, 61] and downstream effectors (YAP and TAZ) [12, 13] of the Hippo pathway are

phosphorylated during mitosis. During these previous studies, we found that the Hippo core kinase MST2 is also phosphorylated during antimitotic drug-induced G2/M phase arrest. In this report, we further characterized the phospho-regulation of MST2 in mitosis and examined the functional significance of the phosphorylation. Our data showed that mitotic phosphorylation inhibits MST2 tumor suppressing activity.

2.2. Materials and Methods

2.2.1. Expression constructs, cell culture and transfection

Flag-MST2 has been described [32]. Point mutations were generated by the QuikChange Site-Directed PCR Mutagenesis Kit (Stratagene) and verified by sequencing. HEK293T, HEK293GP, and HeLa cell lines were purchased from American Type Culture Collection (ATCC) and cultured as ATCC instructed. Attractene (Qiagen) was used for transient overexpression of proteins in HEK293T and HEK293GP cells following the manufacturer's instructions. SiRNA oligos were purchased from Dharmacon (the target sequences were: siMST2-1: CCACAAGCACGA TGAGTGA; siMST2-2: GCCCATATGTTGTAAAGTA; siMST2-3: GAACTTTGGTCCGATGATT) and transfected with HiPerfect reagent from Qiagen (at the final concentration of 40 nM). Transient transfections were done with Attractene reagent (Qiagen) following the manufacturer's instructions. Nocodazole (100 ng/ml for 16h) and Taxol (100nM for 16h) (Selleck Chemicals) were used to arrest cells in G2/M phase. VX680 (Aurora-A,-B, -C inhibitor), BI2536 (PLK1 inhibitor), Purvalanol A (CDK1/2/5 inhibitor), SB216763 (GSK-3 inhibitor) and MK2206 (Akt inhibitor) were also from Selleck Chemicals. RO3306 (CDK1 inhibitor) was from ENZO Life Sciences. Kinase inhibitors for MEK-ERK (U0126) and p38 (SB203580) were from LC Laboratory. All other chemicals were either from Sigma or Thermo Fisher.

2.2.2. Tet-On-inducible expression system

The MST2 or MST2-S385A mutated cDNA was cloned into the Tet-All vector [36] to generate Tet-On-inducible overexpression constructs. Retrovirus packaging, infection, and subsequent selection were done as we have described previously [62]. The transduced cells were selected with neomycin (G418) (400 μg/ml) to establish pooled cell

lines. Cells were maintained in medium containing Tet system-approved fetal bovine serum (Clontech Laboratories).

2.2.3. Recombinant protein purification and in vitro kinase assay

GST-tagged MST2 or MST2-S385A (cloned in pGEX-5X-1) was bacterially expressed and purified on GSTrap FF affinity columns (GE Healthcare) following the manufacturer's instructions. GST-MST2 (1 μg) was incubated with 5–10 U recombinant CDK1/cyclin B complex (New England Biolabs) or 50-100 ng CDK1/cyclin B (SignalChem) in kinase buffer (New England Biolabs) in the presence of 5 μCi γ- ^{32}P-ATP (3000 Ci/mmol, PerkinElmer) as we previously described [15]. Active CDK2, CDK5, p38, JNK1, JNK2, MEK1, ERK1, and PLK1 kinases were also purchased from SignalChem.

2.2.4. Antibodies

Rabbit polyclonal phospho-specific antibodies against human MST2 S385 were generated and purified by AbMart. The peptide used for immunizing rabbits was KRNAT-pS-PQVQR. The corresponding non-phosphorylated peptide was also synthesized and used for antibody purification. Anti-β-actin (SC-47778) and anti-cyclin B (SC-752) antibodies were from Santa Cruz Biotechnology. Glutathione S-transferase (GST) (A190-122A), Mst1 (A300-465A), Mst2 (A300-467A), and Lats1 (A300-478A) antibodies were from Bethyl Laboratories. MST2 antibodies from Cell Signaling Technology (3952) were also used. Phospho-Histone H3 Ser^{10} (3377), phospho- YAP Ser^{127} (4911), phospho-Lats1 Ser^{909} (9157), phospho-Lats1 Ser^{1079} (8654), Phospho-MST1(Thr^{183})/MST2(Thr^{180}) (3681), and cleaved caspase 3 (9664) antibodies were also from Cell Signaling Technology. Anti-PLK1 antibodies were from Biolegend (667701).Phospho-T210 PLK1 antibodies were purchased from BD Bioscience (558400).

2.2.5. Phos-tag and Western blot analysis

Phos-tag™ was obtained from Wako Pure Chemical Industries, Ltd. (304-93521) and used at 20 μM (with 100 μM $MnCl_2$) in 8% SDS-polyacrylamide gels as we previously described [61]. Western blotting, immunoprecipitation, and lambda phosphatase treatment assays were done as previously described [31, 34].

2.2.6. Cell proliferation and colony formation assays

For cell proliferation assays, cells (50,000/well) were seeded in a 6-well plate in triplicate. Cells were counted by a hemacytometer. Colony formation assays in soft agar were performed as described [32]. Cells (5000/well) were seeded in a 6-well plate and colonies were counted by ImageJ online.

2.2.7. Animal studies analysis

For in vivo xenograft studies, 2.0 X 10^6 HeLa cells expressing Tet-All-MST2 or Tet-All-MST2-S385A (non-phosphorylatable mutant) were subcutaneously injected into flanks (both left and right) of 6-week-old male athymic Ncr-nu/nu nude mice (Harlan). Five animals were used per group. Tumor sizes were measured every four days using an electronic caliper starting at 10 days after injection. Tumor volume (V) was calculated by the formula: V = 0.5 X length X $width^2$ [32]. The animals were housed in pathogen-free facilities. All animal experiments were approved by the University of Nebraska Medical Center Institutional Animal Care and Use Committee.

2.2.8. Statistical analysis

Statistical significance was analyzed using a two-tailed, unpaired Student's t-test. Pearson Chi-Square analysis was used to determine the statistical significance in Fig. 2-6C.

2.3. Results

2.3.1. MST2 is phosphorylated during antimitotic drug-induced G2/M arrest

Using a Phos-tag SDS-polyacrylamide gel system, we recently examined the phosphorylation status of the Hippo pathway proteins during G2/M arrest induced by Taxol or Nocodazole. During these experiments, we found that MST2, but not MST1, was upshifted on a SDS-polyacrylamide gel during G2/M arrest (Fig. 2-1A, B) [61]. Lambda phosphatase treatment largely abolished the mobility upshift of MST2, suggesting that MST2 is phosphorylated during G2/M arrest (Fig. 2-1A). The phosphorylation on Thr^{183}-MST1 (Thr^{180}-MST2) in the activation loop was not altered under these conditions (Fig. 2-1B).

2.3.2. Identification of the corresponding kinase for MST2 phosphorylation

We used various kinase inhibitors to identify the candidate kinase for MST2 phosphorylation. Inhibition of p38 kinase (with SB203580), JNK1/2 (with SP600125), MEK-ERK (with U0126), Akt (with MK-2206), PLK1 (with BI2536), Aurora-A, -B, -C (with VX680) or GSK-3 (with SB216763) failed to alter the mobility/phosphorylation of MST2 during G2/M arrest (Fig. 2-1C, lanes 5-11). These inhibitors are effective under the conditions used [12, 63]. Interestingly, treatments with RO3306 (CDK1 inhibitor) or Purvalanol A (CDK1/2/5 inhibitor) almost completely reverted the mobility shift/phosphorylation (Fig. 2-1C, lanes 3-4). These data suggest that CDK1 is likely the corresponding kinase for MST2 phosphorylation induced by Taxol or Nocodazole treatment.

2.3.3. CDK1 phosphorylates MST2 in vitro

Next, we performed in vitro kinase assays with bacterially purified MST2 proteins as substrates to determine which kinase can directly phosphorylate MST2. Fig. 2-2A shows that purified CDK1/cyclin B kinase complex robustly phosphorylated GST-MST2 proteins in vitro (Fig. 2-2A). No or very mild phosphorylation was detected when CDK2, CDK5, p38, JNK1, JNK2, MEK1, or ERK1 kinase was used in these assays, though these kinases recognize the same consensus sequence as CDK1 kinase. These results indicate that CDK1 specifically and directly phosphorylates MST2 in vitro.

2.3.4. CDK1/cyclin B complex phosphorylates MST2 at S385 in vitro

CDK1 phosphorylates substrates at a minimal proline-directed consensus sequence [40]. MST2 only contains a total of 2 S/TP motifs (Ser^{107} and Ser^{385}) and Ser^{107} also exists in MST1. Therefore, Ser^{385} was chosen for further investigation. Interestingly, mutating Ser^{385} to alanine completely abolished the ^{32}P incorporation in GST-MST2, suggesting that Ser^{385} is the main CDK1 site in MST2 in vitro (Fig. 2-2B). A recent report showed that MST2 is also phosphorylated by the mitotic kinase PLK1 [60]. Consistent with that study, we confirmed that MST2 is also a suitable substrate for PLK1 (Fig. 2-2C); however, mutating Ser^{385} to alanine failed to significantly reduce the phosphorylation of MST2 mediated by PLK1 (Fig. 2-2C). These observations suggest that PLK1 and CDK1 phosphorylate different sites in MST2 in vitro.

We have generated phospho-specific antibodies against Ser^{385}. In vitro kinase assays confirmed that CDK1 readily phosphorylates MST2 at Ser^{385} (Fig. 2-2D). Mutating Ser^{385} to alanine abolished the phosphorylation, confirming the specificity of our antibody (Fig. 2-2D). These data indicate that CDK1 phosphorylates MST2 at Ser^{385} in vitro.

2.3.5. CDK1 phosphorylates MST2 at S385 in cells

Next, we explored whether this phosphorylation occurs in cells. Taxol treatment significantly increased the phosphorylation of MST2 Ser^{385} (Fig. 2-3A). Addition of RO3306 or Purvalanol A, but not the PLK1 kinase inhibitor BI2536, greatly inhibited MST2 Ser^{385} phosphorylation, suggesting that these antibodies specifically recognize phosphorylated MST2 and that phosphorylation of MST2 Ser^{385} is CDK1 kinase dependent (Fig. 2-3A). As expected, the signal of MST2 Ser^{385} was significantly reduced in MST2 knockdown cells (Fig. 2-3B). Using immunoprecipitated samples, we further demonstrated that MST2 is phosphorylated on Ser^{385} during Taxol-induced G2/M in a CDK1-dependent manner (Fig. 2-3C).

2.3.6. MST2 phosphorylation on Ser^{385} occurs during normal mitosis

To determine whether phosphorylation of MST2 Ser^{385} occurs during normal mitosis, a double thymidine block and release method was used [38]. Fig. 2-3D shows that the p-MST2 S385 signal was significantly increased in cells after 11 h of being released from double thymidine block (Fig. 2-3D). A significant portion of cells is in mitosis, as revealed by increased cyclin B levels (Fig. 2-3D). These results indicate that the phosphorylation of MST2 S385 occurs dynamically during normal mitosis.

2.3.7. Mitotic phosphorylation of MST2 does not impact Hippo-YAP activity

MST2 is a core kinase in the Hippo-YAP signaling. We first tested whether this phosphorylation affects its kinase activity. The non-phosphorylatable (MST2-S385A) mutant has similar basal kinase activity revealed by phosphorylation at T180 as wild type MST2 (Fig. 2-4A), suggesting that S385 phosphorylation of MST2 does not impact its kinase activity. As expected, YAP S127 (a major phosphorylation site mediated by

LATS1/2 kinases) phosphorylation was significantly increased upon MST2 overexpression [32, 62]. However, ectopic expression of MST2-S385A had similar effects as wild type MST2 on YAP S127 phosphorylation (Fig. 2-4B). We further established doxycycline-induced MST2 or MST2-S385A in HeLa cells, and in the presence of doxycycline, both wild type MST2 and MST-S385A were modestly induced at a similar level (Fig. 2-4C). No significant changes were detected in the Hippo-YAP signaling activity under these conditions (Fig. 2-4C). These observations suggest that phosphorylation of MST2 at S385 does not affect Hippo-YAP activity.

2.3.8. The non-phosphorylatable mutant MST2 possesses stronger inhibitory activity in cell proliferation and anchorage-independent growth

Next, we compared the effects from doxycycline-induced MST2- or MST2-S385A-expressing HeLa cells to determine the biological significance of S385 phosphorylation of MST2. Interestingly, overexpression of the MST2-S385A mutant significantly reduced cell proliferation when compared to MST2-expressing cells (Fig. 2-5A). Furthermore, MST2-S385A-expressing cells formed a significantly lower number of colonies in soft agar when compared with MST2-expressing cells (Fig. 2-5B, C). These data suggest that mitotic phosphorylation inhibits MST2 activity in suppressing cell proliferation and anchorage-independent growth.

2.3.9. The non-phosphorylatable MST2 mutant inhibits tumorigenesis in vivo

We further evaluated the influence of S385 phosphorylation on tumor growth in animals. An equal number of HeLa cells expressing MST2 or MST2-S385A were subcutaneously inoculated into immunodeficient mice and tumor size was monitored in the presence of doxycycline. Interestingly, in line with the results in Fig. 2-5, tumors from mice bearing MST2-S385A-expressing cells were significantly smaller when compared

with those from mice injected with wild type MST2- expressing cells (Fig. 2-6A, B). Western blotting analysis showed that MST2 (wild type or S385A) expression levels were similar in most of these tumors (Fig. 2-6C). Interestingly, expression of MST2-S385A induced stronger apoptosis (detected by cleaved caspase 3) when compared with wild type MST2 (Fig. 2-6C, Pearson Chi-Square test, $p<0.1$). These results suggest that phosphorylation of MST2 at S385 inhibits its tumor suppressing activity in vivo.

2.4. Discussion

In the current study, we identified a novel phosphorylation site (S385) on MST2 that is dynamically/transiently phosphorylated by CDK1 during mitosis. The mitotic phosphorylation of MST2 inhibits its tumor suppressing activity without affecting its own kinase activity and the Hippo-YAP signaling. Together, we provided a novel layer of regulation of MST2 activity in cancer cells.

MST2 along with WW45 plays a pivotal role in centrosome disjunction. They directly interact with NIMA-related kinase Nek2A and recruit it to the centrosome [45]. Specifically, MST2 phosphorylates Nek2A and consequently promotes its recruitments to the centrosome. Further, the MST2-WW45 complex contributes to the phosphorylation of the c-Nap1 and Rootletin (two centrosomal linker proteins) which are major Nek2A phosphorylation targets and bridge the gap between the two centrosomes. Interestingly, other Hippo pathway components, such as LATS1/2, Rassf1A and YAP are dispensable for Nek2A recruitment [45]. Those phenotypes are compatible with MST2 S385 phosphorylation. They affect mitosis without impacting Hippo-YAP activity. Whether S385 phosphorylation of MST2 is involved in this process is still unknown.

On the other hand, down regulation of MST2 causes chromosome misalignment mediated by Aurora B [59]. Besides, MST2 cooperates with its activator, Mob2 and a scaffold protein, Furry, to contribute to mitotic activation of NDR1 kinase, thereby regulating the precise alignment of mitotic chromosomes [64].

Taken together, MST2 is essential in centrosome regulation and chromosome alignment in mitosis. Future studies are needed to further determine whether S385 phosphorylation of MST2 contributes to the fidelity of mitosis and how this phosphorylation links subsequent tumorigenesis. Our results showed that mitotic phosphorylation of MST2

S385 does not impact the LATS and YAP activity and thus, it will be interesting to see what the downstream effector of S385 phosphorylation is.

Figure 2-1. CDK1-dependentphosphorylation of MST2 duringG2/M arrest.

(A) HeLa cells were treated with Taxol as indicated and cell lysates were further treated with (+) or without (-) λ phosphatase (ppase). Total cell lysates were probed with anti-MST2 antibody on Phos-tag SDS-polyacrylamide gels. (B) HeLa cells were treated with DMSO, Taxol or Nocodazole (Noco). Total cell lysates were probed with the indicated antibodies on Phos-tag or regular SDS-polyacrylamidegels. (C) HeLa cells were treated with Taxol together with or without various kinase inhibitors as indicated. RO3306 (CDK1 inhibitor, 5μM), Purvalanol A (CDK1/2/5 inhibitor, 10 μM), SB203580 (p38 inhibitor, 10 μM), SP600125 (JNK1/2 inhibitor, 20μM), U0126 (MEK-ERK inhibitor, 20 μM), MK2206 (AKT inhibitor, 10 μM), BI2536 (PLK1 inhibitor, 100 nM), VX680 (Aurora-A, B, C inhibitor, 2 μM), and SB216763 (GSK3 inhibitor, 10 μM) were used. Inhibitors were added 1-2h before harvesting the cells (with MG132toprevent cyclin B from degradation and cells from exiting from mitosis). Total cell lysates were subjected to Western blotting with the indicated antibodies. SE: short exposure; LE: long exposure.

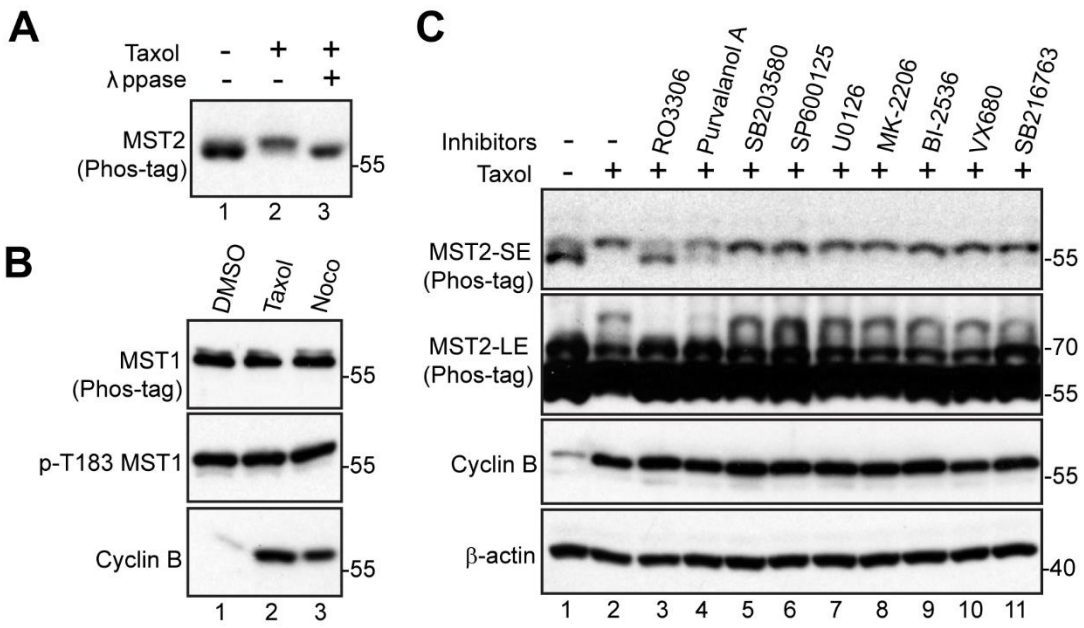
A
Taxol - + +
λppase - - +
MST2
(Phos-tag)
-55
1 2 3
B
DMSO
Taxol
Noco
MST1
(Phos-tag)
-55
p-T183 MST1
-55
Cyclin B
-55
1 2 3
C
Inhibitors - - RO3306 Purvalanol A SB203580 SP600125 U0126 MK-2206 BI-2536 VX680 SB216763
Taxol - + + + + + + + + + +
MST2-SE
(Phos-tag)
-55
MST2-LE
(Phos-tag)
-70
-55
Cyclin B
-55
β-actin
-40
1 2 3 4 5 6 7 8 9 10 11

Figure 2-2. CDK1 phosphorylates MST2 in vitro.

(A) In vitro kinase assays with kinases as indicated. (B) In vitro kinase assays with CDK1/cyclin B complex using GST-MST2 or GST-MSTS385A proteins as substrates. RO3306 (5μM) was used to inhibit CDK1 kinase activity. (C) In vitro kinase assays with PLK1 kinase using GST-MST2 or GST-MSTS385A proteins as substrates. (D) In vitro kinase assays were done as in B except anti-p-S385 MST2 antibody was used.

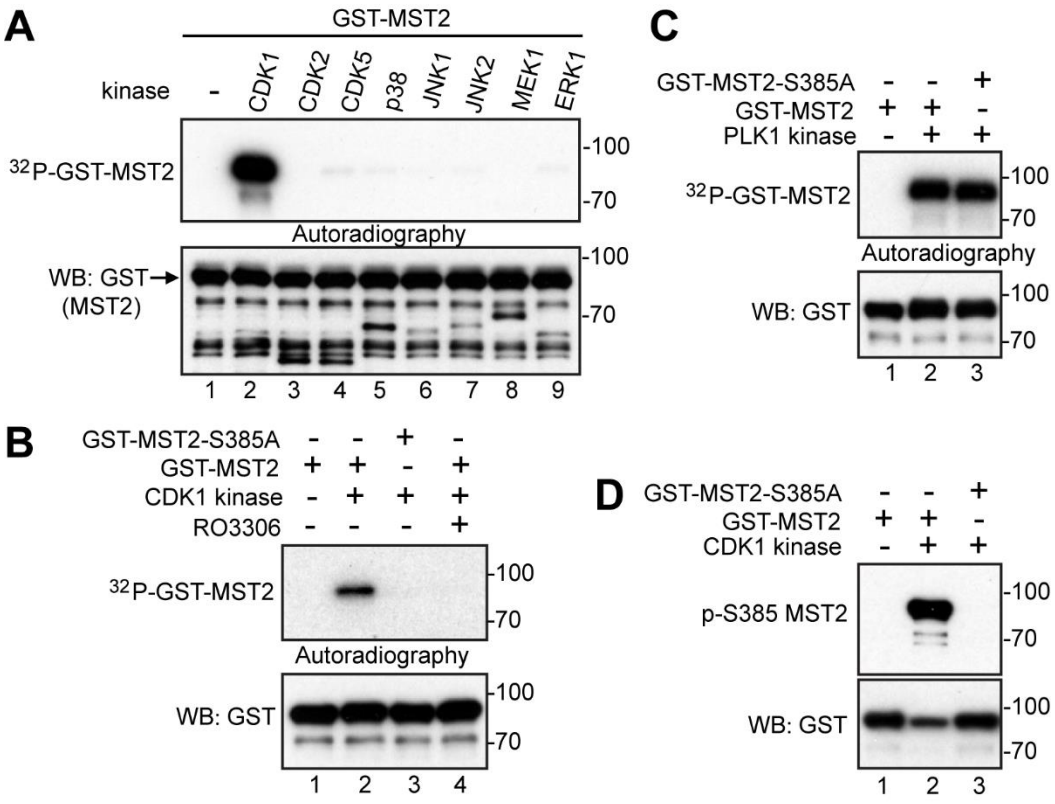
A
GST-MST2
kinase
-
CDK1
CDK2
CDK5
p38
JNK1
JNK2
MEK1
ERK1
32P-GST-MST2
Autoradiography
WB: GST
(MST2)
100
70
1 2 3 4 5 6 7 8 9
B
GST-MST2-S385A
GST-MST2
CDK1 kinase
RO3306
32P-GST-MST2
Autoradiography
WB: GST
1 2 3 4
C
GST-MST2-S385A
GST-MST2
PLK1 kinase
32P-GST-MST2
Autoradiography
WB: GST
1 2 3
D
GST-MST2-S385A
GST-MST2
CDK1 kinase
p-S385 MST2
WB: GST
1 2 3

Figure 2-3. CDK1 mediates the phosphorylation of MST2 S385 in cells.

(A) HeLa cells were treated with Taxol together with or without various kinase inhibitors as indicated. Inhibitors were added 1.5 h before harvesting the cells (with MG132 to prevent cyclin B from degradation and cells from exiting from mitosis). Total cell lysates were subjected to Western blotting with the indicated antibodies. (B) HeLa cells were transfected with scrambled siRNA (control) or siRNA against MST2 for 48h and were further treated with (+) or without (-) Taxol for 14h. The total cell lysates were subjected to Western blotting with the indicated antibodies. (C) MST2 proteins in HeLa cells were immunoprecipitated and the samples were probed with phospho-S385 MST2 and subsequent MST2 antibodies. Total lysates before immunoprecipitation were also probed with the indicated antibodies. CDK1 inhibitors RO3306 (5 μM) or Purvalanol A (10 μM) together with MG132 (25 μM) were added 1.5 h before the cells were lysed. * marks the IgG heavy chain. (D) A double thymidine block and release was performed in HeLa cells and samples were collected at the indicated time points. The total cell lysates were probed with the indicated antibodies.

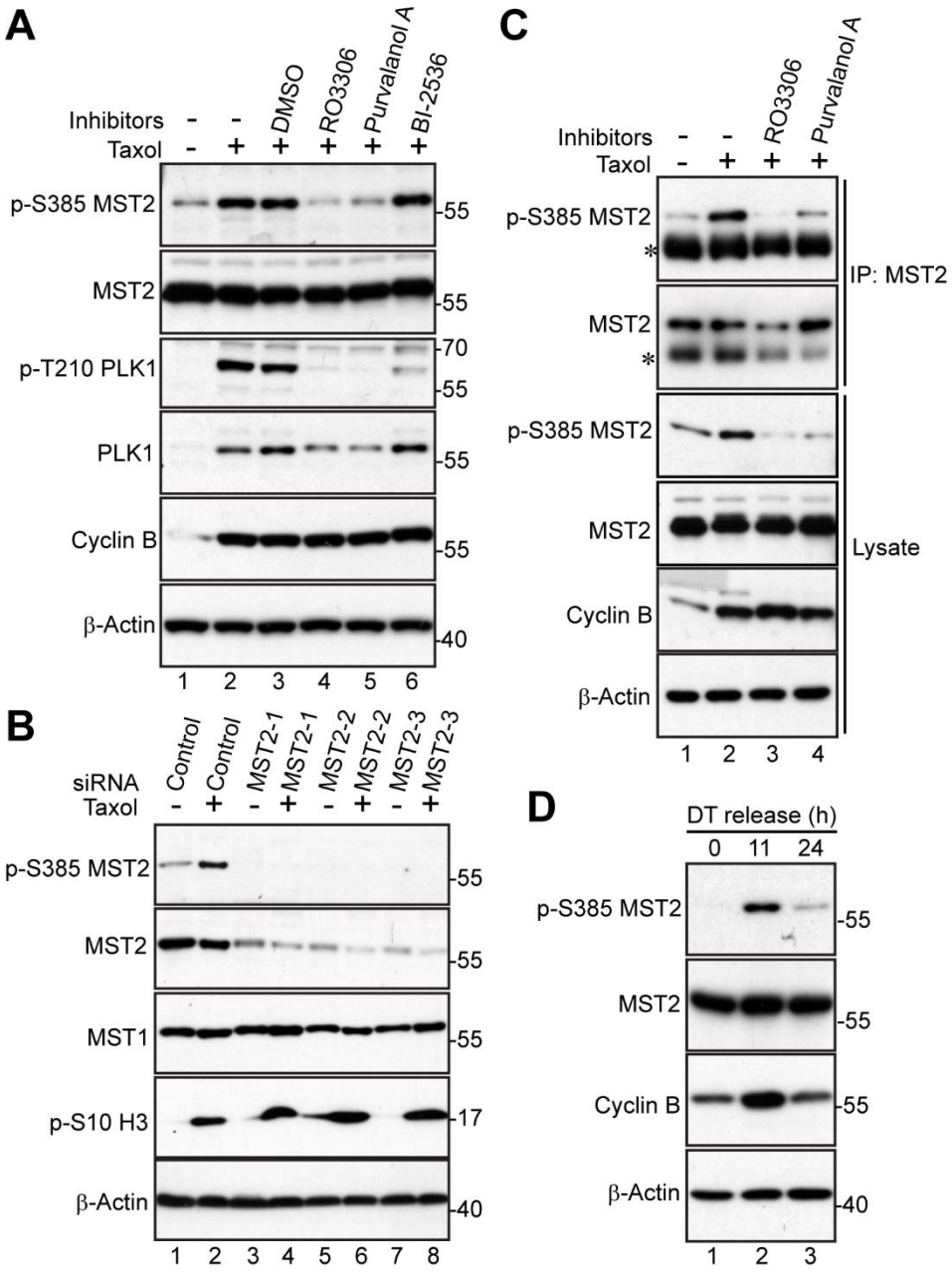
A
Inhibitors - - DMSO RO3306 Purvalanol A BI-2536
Taxol - + + + + +
p-S385 MST2
MST2
p-T210 PLK1
PLK1
Cyclin B
β-Actin
55
55
70
55
55
55
40
1 2 3 4 5 6
B
siRNA Control Control MST2-1 MST2-1 MST2-2 MST2-2 MST2-3 MST2-3
Taxol - + - + - + - +
p-S385 MST2
MST2
MST1
p-S10 H3
β-Actin
55
55
55
17
40
1 2 3 4 5 6 7 8
C
Inhibitors - - RO3306 Purvalanol A
Taxol - + + +
p-S385 MST2
*
MST2
*
IP: MST2
p-S385 MST2
MST2
Cyclin B
β-Actin
Lysate
1 2 3 4
D
DT release (h)
0 11 24
p-S385 MST2
MST2
Cyclin B
β-Actin
55
55
55
40
1 2 3

Figure 2-4. Mitotic phosphorylation of MST2 does not affect the Hippo-YAP activity.

(A) HEK293T cells were transfected with Flag-MST2 or Flag-MST2-S385A as indicated. The immunoprecipitates (with Flag antibodies) were probed with the indicated antibodies. * marks the IgG heavy chain. WT: wild type. (B) GFP-YAP was co-transfected with Flag-MST2-WT or Flag-MST2-S385A with or without Flag-LATS2. The cells were harvested at 48 h post-transfection and the total cell lysates were analyzed by Western blotting with the indicated antibodies. (C) Establishment of Tet-On-inducible HeLa cell lines expressing vector, MST2-WT, or MST2-S385A. Total cell lysates were harvested from these cell lines in the presence of doxycycline (1 μg/ml for 2 days) and were subjected to Western blotting analysis.

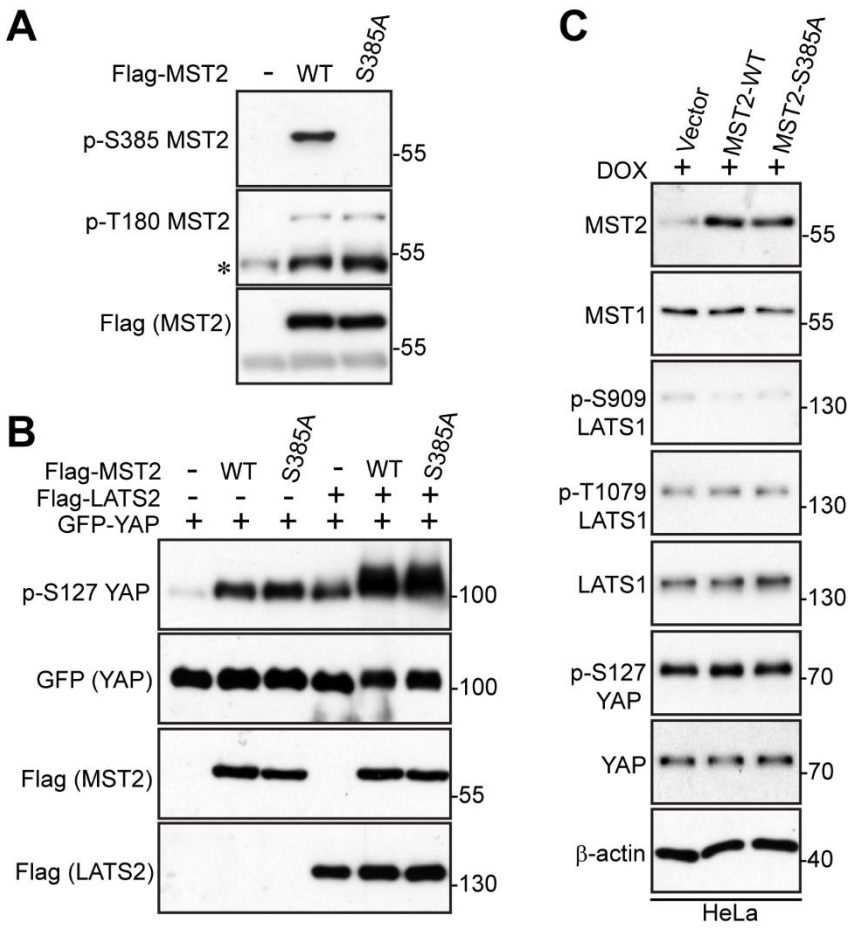
A
Flag-MST2 - WT S385A
p-S385 MST2
p-T180 MST2
*
Flag (MST2)
55
55
55
B
Flag-MST2 - WT S385A - WT S385A
Flag-LATS2 - - - + + +
GFP-YAP + + + + + +
p-S127 YAP
GFP (YAP)
Flag (MST2)
Flag (LATS2)
100
100
55
130
C
Vector
MST2-WT
MST2-S385A
DOX + + +
MST2
MST1
p-S909 LATS1
p-T1079 LATS1
LATS1
p-S127 YAP
YAP
β-actin
55
55
130
130
130
70
70
40
HeLa

Figure 2-5. MST2-S385A suppresses cell proliferation and anchorage-independent growth.

(A) Cell proliferation assays with HeLa cells-expressing Tet-MST2-WT or Tet-MST2-S385A. Cells were kept on Tet-approved FBS and doxycycline was added (1 μg/ml) to the cells 2 days prior to the experiments. Data were expressed as the mean ± s.d. of three independent experiments. **: $p < 0.01$; *: $p < 0.05$ (t-test). (B, C) Colony assays in soft agar to assess anchorage-independent growth of HeLa cells expressing Tet-MST2-WT or Tet-MST2-S385A in the presence of doxycycline. Data were expressed as the mean ± s.d. of three repeats (B) and representative images were shown (C). **: $p < 0.01$ (t-test). WT: wild type.

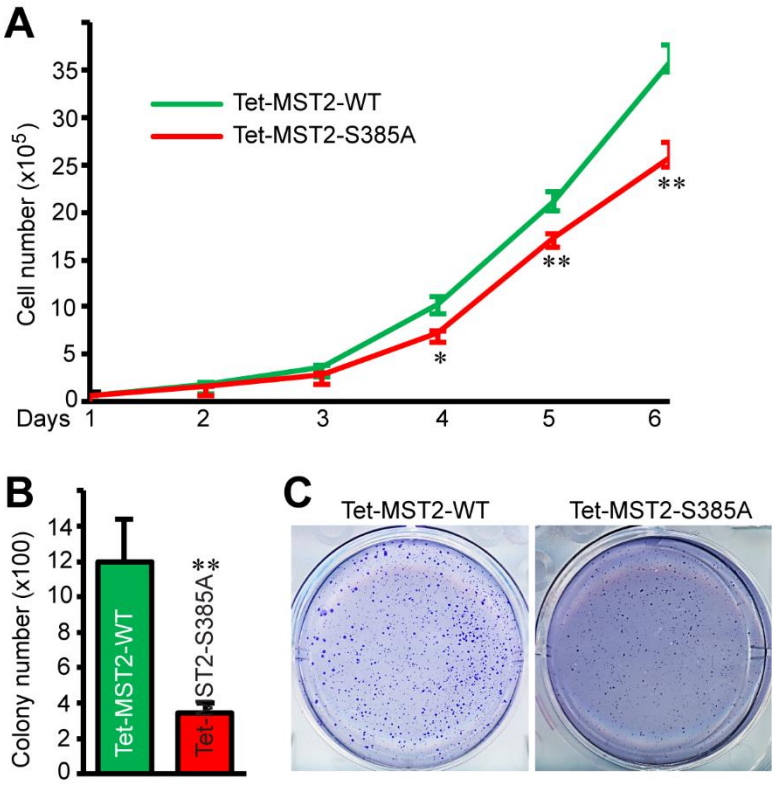
A
Cell number (x10^5)
35
30
25
20
15
10
5
0
Days 1
2
3
4
5
6
Tet-MST2-WT
Tet-MST2-S385A
*
**
**
B
Colony number (x100)
14
12
10
8
6
4
2
0
Tet-MST2-WT
Tet-MST2-S385A
**
C
Tet-MST2-WT
Tet-MST2-S385A

Figure 2-6. MST2-S385A suppresses tumorigenesis in mice.

(A) Tumor growth curve. HeLa cells expressing Tet-MST2-WT or Tet-MST2-S385A were subcutaneously inoculated into athymic nude mice (n = 5, on both left and right flanks) and the mice were kept on doxycycline (0.5 mg/ml)-containing water throughout the experiments. One inoculation (left flank) in the wild type group did not form visible tumor and was excluded from the analysis. Therefore, the tumor volume at each point was the average of 9 (MST2-WT) or 10 (MST2-S385A) tumors. **: $p< 0.01$; *: $p < 0.05$ (t-test). (B) The tumors in each group were excised and photographed at the endpoint. (C) Western blotting analysis with tumor samples from B. Pearson Chi-Square test showed that it was marginally significant between two groups ($p < 0.1$).wild type.

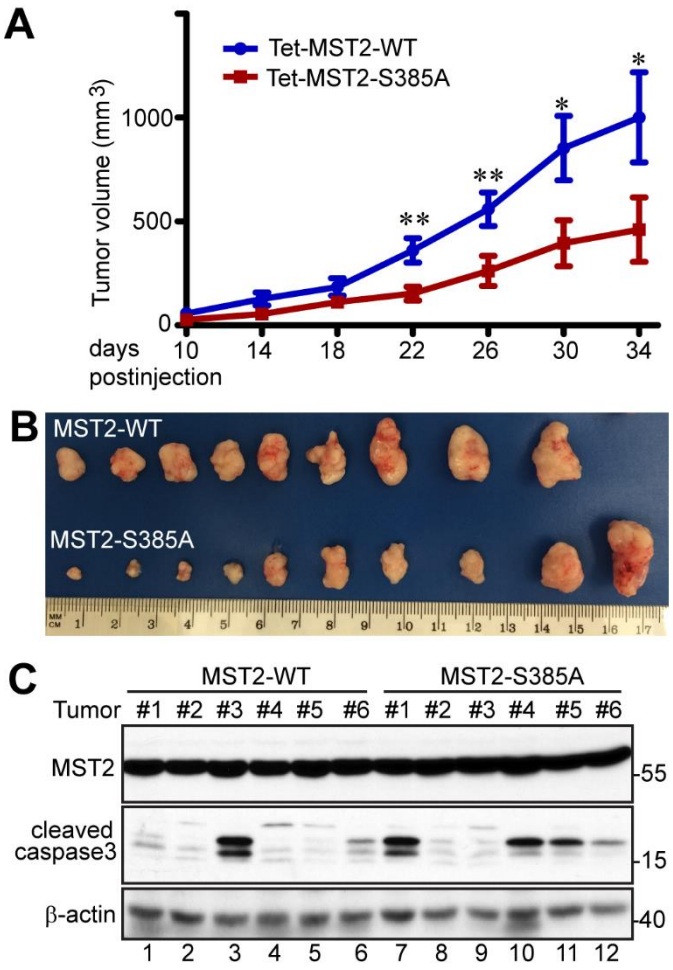
A
Tet-MST2-WT
Tet-MST2-S385A
Tumor volume (mm3)
1000
500
0
days postinjection
10
14
18
22
26
30
34
**
**
*
*
B
MST2-WT
MST2-S385A
C
MST2-WT
MST2-S385A
Tumor #1 #2 #3 #4 #5 #6 #1 #2 #3 #4 #5 #6
MST2
cleaved caspase3
β-actin
55
15
40
1 2 3 4 5 6 7 8 9 10 11 12

CHAPTER 3: ROLE OF YAP IN PANCREATIC CANCER-ASSOCIATED CACHEXIA

ABSTRACT

Cachexia is a wasting syndrome characterized by body weight loss, atrophy of white adipose tissue, and systemic inflammation. It frequently occurs in patients of infectious diseases, such as AIDS and tuberculosis, or chronic disease, like heart failure, pulmonary disease and chronic kidney disease. Most commonly, cachexia is observed in cancer, termed cancer-associated cachexia (CAC). Pancreatic cancer has one of the highest incidences of cachexia compared to other cancer types. Pancreatic ductal adenocarcinoma (PDAC), is one of the devastating diseases that causes a high death rate worldwide. Last decade, the Hippo-YAP signaling pathway was discovered and identified as a tumor suppressor pathway, via controlling cell proliferation and apoptosis. Recent studies indicate that Hippo-YAP signaling plays a critical role in the development of pancreatic cancer. However, the underlying mechanism is poorly understood and furthermore, little is known whether YAP is involved in pancreatic CAC. To address these important questions, we generated a doxycycline-inducible mouse model in which active YAP was specifically expressed in the pancreas to explore the role of YAP and underlying mechanisms in the development of pancreatic CAC. We observed that pancreatic specific activation of YAP in mice leads to pancreatic acinar-to-ductal metaplasia (ADM) in two weeks. Moreover, significant body weight loss and food intake decrease were observed after YAP induction in the pancreas. Further, we showed that the level of CXCL13 was increased in serum of YAP-pancreas mouse model. Thus, our study suggests a potential role of the YAP-CXCL13 axis in pancreatic CAC.

3.1. Introduction

It is estimated that half of cancer patients develop cachexia syndrome at their late stage with a severe loss of adipose tissue and skeletal muscle mass [65]. Cachexia is characterized by body weight loss, atrophy of white adipose tissue, and systemic inflammation. Limited treatment is currently available for cancer-associated cachexia (CAC), which leads to approximately 20% of total deaths in cancer patients [66]. Therefore, new therapeutic targets for CAC prevention and treatment are urgently needed.

In the past decades, the investigators have searched for potential mediators of CAC in hoping to develop therapeutic strategies against tumor induced weight loss and muscle atrophy. The loss of body fat seems to arise from the increased lipolysis, not the decreases of lipogenesis. This idea was confirmed by the result of elevated level of free fatty acids (FFA) and glycerol in cachexia cancer patient plasma, even presented before significant weight loss [67]. In addition to lipolysis increase, there is a well-established link between cachexia and systematic inflammation. Interleukin 6 (IL-6) acts alone, or correlated with other cytokines, as a driver of systematic inflammation in CAC [68]. Circulating levels of IL-6 have been shown to correlate with weight loss, as well as survival in cancer patients [69]. In an IL-6-proficent murine synergetic model of cachexia, the silencing of IL-6 could rescue the cachexia phenotype, including the reduction of loss of fat tissue and morphology change of adipose tissue. The anti-IL-6 antibody treatment can protect K5-SOS cachexia mice model from losing fat, but recent clinical trials of a monoclonal anti-IL-6 antibody in weight-losing lung cancer patients have no significant effect on loss of body mass [70, 71]. However, the antibody treatment on patients showed reversal of anorexia, fatigue, and anemia [72]. Therefore, additional potential targets for CAC treatment is urgently needed. What these targets are and how they contribute to CAC are critical subjects for current investigation.

Cachexia is associated with multiple type of cancers, particularly the gastrointestinal tract cancer and the lung cancer [73]. Among those cancer types, PDAC has the highest incidence of cancer cachexia and patients experience the greatest degree of weight loss and shorter survival time [74]. Pancreatic intraepithelial neoplasia (PanIN) is responsible for the development of pancreatic cancer. The origin of the duct cell in the PanIN-PDAC progression model is compatible with the concept of acinar to ductal metaplasia (ADM) preceding the generation of ~~the~~ small ducts [75].

The Hippo-YAP signaling pathway was originally discovered in Drosophila and plays an important role in tumorigenesis by regulating cell proliferation and apoptosis [2]. Later studies showed that this pathway is highly conserved in mammals [76, 77]. The classic pathway in mammals consists of a series of kinases cascade. The core components of the Hippo pathway contain kinases MST1/2 (mammalian sterile-20 like kinases1/2) and LATS1/2 (large tumor suppressor 1/2), with two scaffold proteins Sav (Protein Salvador Homolog 1) and Mob1 (Mps one binder 1). MST1/2 directly phosphorylates LATS1/2 to activate LATS1/2, which subsequently phosphorylate and inhibit the downstream effector YAP (yes-associated protein) and TAZ (transcriptional co-activator with PDZ binding domain). Without the inhibition of Hippo signaling, YAP/TAZ can translocate from cytoplasm to nucleus. After binding with transcription factors, transcription of target genes will be induced to promote cell proliferation and inhibit apoptosis [7]. Studies from mouse models and cancer patients confirmed/demonstrated the oncogenic role of YAP in tumorigenesis. For example, overexpression of YAP specifically in liver is sufficient to promote hepatocellular carcinoma within three months [32]. Half of aged prostate-specific YAP transgenic mice are able to develop prostate tumors compared with no tumor formed in the wildtype control [78]. These mouse model studies suggest that YAP plays an important role in cancer development.

Recent studies suggested that YAP also plays significant role in the development of pancreatic cancer. In our previous study, upregulation of YAP in pancreatic cells can promote pancreatic cancer cell migration and invasion *in vitro* [79]. Additionally, hyperactive YAP in pancreatic cell not only promotes anchorage-independent growth *in vitro*, but also drives tumorigenesis in xenograft mice [79]. Furthermore, Kapoor et al. showed that YAP activation can maintain tumor growth in Kras (G12D)-driven PDAC model upon KRAS extinction [80]. These lines of evidence indicate that the transcriptional co-activator YAP plays an important role in pancreatic cancer development. We further explore the role of YAP in PDAC by generating intact transgenic animals, which was the first transgenic animal model expressing hyperactive YAP specifically in pancreas. Our study showed that the YAP-pancreas mouse not only initiated ADM, but also caused severe weight loss and food intake reduction. Further, we observed highly elevated serum level of CXCL13 in YAP-pancreas mouse, indicating the potential role of this cytokine in cachexia development.

3.2. Materials and Methods

3.2.1. Generation of mouse strains

Genetically engineered mouse strains TetO-YAP^{S127A} [81], Ptf1α-Cre (Mutant Mouse Resource & Research Centers) and Rosa-LSL-rtTA (Jackson Lab) were interbred to generate all experimental colonies (Fig 3-1). All the experimental animals were maintained on mixed background in pathogen-free conditions at University of Nebraska Medical Center (UNMC). Mice were fed with doxycycline water (Doxycycline Hyclate, Sigma-Aldrich D9891, 0.2mg/ml in 25mg/ml sucrose) to induce active YAP expression specifically in pancreas. All manipulations were approved under UNMC Institutional Animal Care and Use Committee (IACUC) under protocol number 12-044.

3.2.2. Cachexia phenotype observation/measurement

Each group (control and YAP transgenic) has equal amount (n=3) of mice which were housed in the cage with same size. Total body weight was measured at time point of 1 week and 8 weeks after Dox induction. For Food intake measurements, equal amount of food tablets was dispensed to each group at the beginning of the designed week. The weight of given food tablets were measured same time everyday within the designed week. Average food intake of each mice within the week were calculated.

3.2.3. Immunohistochemistry (IHC) Staining

Tissues were fixed in 4% formalin overnight and embedded in paraffin. The unstained slides were deparaffinized in xylene and hydrated gradually. The hydrated slides were treated with standard citrate or tris-EDTA retrieval buffer for 30 min at 95°C. After incubation overnight with the primary antibodies at 4°C, the slides were incubated with biotinylated secondary antibodies (VECTASTAIN Elite ABC HRP Kit, PK-6100, Vector

Laboratories Ltd.) for 30 min at room temperature. Antibody labeling was visualized with a DAB kit follow the manufacturer's instructions (ImmPACT DAB Peroxidase HRP Substrate, Vector Laboratories Ltd). The antibodies used for IHC analyses are shown below. YAP (1:1000 dilution, 4912), Keratin 17/19 (1:200 dilution, 12434), and α-Amylase (1:300 dilution, 3796) were from Cell Signaling Technology. Ki67 (1:400 dilution, PA5-16785) is from Thermo Fisher.

3.2.4. Analysis of secreted cytokines and CXCL13 ELISA measurements

The mouse blood samples were collected at designed time point. Samples clotted for 2 hours at room temperature before centrifuging for 20 minutes at 2000 x g. Serum were collected for assay immediately or aliquoted and stored at -80°C. Avoid repeated freeze-thaw cycles. Semiquantitative cytokine detection was performed using Proteome Profiler Antibody Arrays for 111 different antibodies (R&D system; ARY028) according to manufacturer's instructions. The CXCL13 level was measured using mouse CXCL13 ELISA kits (R&D system; MCX130) [71].

3.2.5. Statistical analysis

Data were analyzed via two-tailed and unpaired Student's t test or ANOVA. $P < 0.05$ was considered statistically significant.

3.3. Results

3.3.1. YAP is sufficient to promote ADM in YAP-pancreas model.

Previous studies have demonstrated in immunodeficiency mice that YAP gain-of-function can promote pancreatic cancer cell tumorigenesis [79]. However, there is no transgenic mouse model available to further explore the role of YAP in pancreatic cancer. To determine whether YAP is involved in PDAC oncogenesis, we obtained the following mouse strains, TetO-YAP^{S127A} [81], Ptf1α-Cre (Mutant Mouse Resource & Research Centers) and Rosa-LSL-rtTA (Jackson Lab) from colleagues (Table 1). Using mouse strains above, for the first time, we established pancreas-specific dox-inducible YAP overexpression transgenic mouse model (Fig 3-1). PDAC are thought to originate from mature acinar cells which will transdifferentiate into ductal-like cells, a process known as acinar to ductal metaplasia (ADM). When YAP-transgenic mice (1-month-old) were exposed to Dox for 2 weeks, they developed ADM. YAP-overexpressed pancreases were distinguishable from wild-type pancreas in overall histology by hematoxylin and eosin (H&E), major pancreatic cell lineage markers [including amylase (in acinar cells), cytokeratin 19 (CK19; in ductal cell)], and the proliferation marker (Ki67). Generally, the H&E staining indicates that most area of wild-type pancreas have normal acinar cell presented, while the examination of pancreatic tissues from young YAP-pancreas transgenic mice showed abnormal cell morphology (Fig 3-2A). Further, the IHC staining showed that YAP overexpression pancreas significantly increased duct-like area (CK19+) but have fewer acinar cell area (α-Amylase+) compared with wild-type pancreas (Fig 3-2B). Additionally, those ductal-like area of YAP-pancreas transgenic mice showed high level of YAP and Ki67 expression, indicating that YAP activation promoted cell proliferation and ADM in pancreas. (Fig 3-2A). Comparing the size and texture of pancreas in control and transgenic mice, the pancreases from the transgenic group were enlarged and of

elastic, hard consistency (Fig 3-2C). Those observations indicate that the acinar cells have been transdifferentiated into ductal-like cells in YAP-pancreas transgenic mice. These results suggest that the specific expression of YAP in pancreas initiates the process of ADM, which can finally develop to PDAC.

3.3.2. The YAP-pancreas model has cachectic phenotype.

Cachexia is a wasting syndrome characterized by body weight loss, atrophy of white adipose tissue, and systemic inflammation [67, 72, 82]. Besides the ADM, we also observed cachectic phenotype on the YAP-Pancreas model. After being exposed to dox for 8 weeks, the 3-month-old YAP-pancreas transgenic model displayed a loss of 15% to 30% of total body weight (Fig 3-3A). Food intake was decreased in both female and male transgenic mice, (Fig 3-3B, 3C). At necropsy, YAP-pancreas model exhibited massive fat atrophy, as evidenced by almost complete loss of gonadal fat (Fig 3-3D). Histological examination of gonadal fat revealed the presence of abundant islets composed of small adipocytes with big nuclei and multilocular cytoplasm (Fig 3-3E). These data indicate that YAP overexpression in pancreas has the potential to promote CAC.

3.3.3. Association between YAP and CXCL13 in pancreatic CAC.

Serum levels of many cytokines and their soluble receptors are manipulated in diverse cancer types [83]. The mutual effect between cancer cell and its microenvironment can induce further production and release of cytokines. Several cytokines including TNF–α, IL-6 have been reported in facilitating a cachectic state [83, 84]. According to known characteristics of CAC and our results, we expect that high level of YAP in pancreas tumor will stimulate the induction of tumor-derived cytokines (tumorkines). Proteome Profiler Mouse Cytokine Array Kit (R&D) was applied to detect the level of 111 cytokines with single plasma sample (Fig 3-4A). We found that the level of several cytokines

(CCL17/TARC 2, CHI3L1 , CXCL13, CXCL16 , LDL R , Lipocalin-2/NGAL, Pentraxin 2/SAP 2 and Pentraxin 3/TSG-14) were significantly elevated after YAP induction (Fig 3-4A, 4B). Further, we examined the serum level of CXCL13 in YAP-pancreas model and control mice with both 1 week and 1 month dox induction via CXCL13 ELISA kit. The upregulation of CXCL13 in the YAP-pancreas model was confirmed (Fig 3-4C).

3.4. Discussion

Recent studies demonstrated that YAP gain-of-function promotes pancreatic cancer cell tumorigenesis *in vitro* and *in vivo* (both subcutaneously and orthotopically) [79, 80]. We then established genetically engineered mouse model of pancreas-specific YAP overexpression. In this study, the genetic mouse model we generated displayed ADM and cachectic phenotype (Fig 3-2, 3). We further identified the high level cytokine, CXCL13, in the mouse model serum via cytokine array (Fig 3-4). The role of CXCL13 in pancreatic cancer and cachexia will be determined in future study.

CXCL13 is a small cytokine belonging to the CXC chemokine family, also known as B cell-attracting chemokine 1 (BCA-1). It is expressed by stromal cells within B-cell follicles in secondary lymphoid tissues [85]. Tumor-infiltrating lymphocyte B cells have been reported to be prevalent in human pancreatic cancer tissues [86]. B cell infiltration was detected by Pylayeva-Gupta et al in human PanIN and Kras-driven pancreatic cancer model [87]. This group further showed implanted pancreatic ductal epithelial cells expressing oncogenic KrasG12D into wild-type pancreata induced B cells accumulation in the regions of neoplastic lesions. Besides, the implantation using mice lacking B cells (μMT mice) had reduced tumor growth compared with tumors grown in wild-type mice. Meanwhile, the anti-CXCL13 treatment can also reduce tumors grown in implantation [87]. These studies identified a B-cell subset that infiltrates into pancreas during early neoplasia and is essential for pancreatic tumorigenesis.

To date, the role of Tumor-infiltrating lymphocytic B cells (TIL-Bs) in PDAC has not been widely investigated. Based on recent publications, the infiltration of B cell supports pancreatic tumorigenesis through multiple mechanisms, including suppression of other immune cells in the tumor microenvironment and promoting pancreatic cancer cell proliferation. Inhibition of B-cell infiltration into the tumor, inhibition of B-cell activity, or

simple depletion of B cells using a specific mAb significantly reduced tumor progression [71, 86]. A clinical study showed that the serum level of B cell-activating factors in pancreatic cancer patients is associated with survival, and maturation of B cells was significantly higher in pancreatic cancer patients than in healthy subjects [88].

The Hippo-YAP signaling pathway was originally discovered in Drosophila and plays an important role in tumorigenesis by regulating cell proliferation and apoptosis [2]. Both in vitro cell study and in vivo immunodeficiency mice study showed that the loss of LATS1/2 promoted cell proliferation and tumor survival. However, the loss of LATS1/2 suppressed tumor growth in animal with intact immune system which demonstrates its ability to stimulate an immune response leading to the destroying of cancer cells [89]. However, Guo et al reported later that activation of YAP in tumor-initiating cells (TICs) recruits macrophage to small foci of altered hepatocytes. The recruitment is mediated by secreted chemokine CCL2 and growth factor CSF1 induced by YAP-TEAD transcriptional complex. Elimination of TIC-associated macrophages (TICAMs) impede tumorigenesis [90]. Interestingly, YAP mediates myeloid-derived suppressor cells (MDSC) infiltrating to prostate tumor via activation of CXCL5-CXCR2 signaling. The infiltrated MDSC promotes prostate tumor progression [91]. The role of Hippo pathway in cancer immune is still under debate. Based on published discoveries, the activation of its downstream effector YAP or knock-out of its upstream kinase will induce immune response via different mechanisms depending on experimental models. Meanwhile, the activity of YAP was recently reported to be regulated by metabolic pathways, such as aerobic glycolysis and mevalonate synthesis [10, 92, 93]. In the meantime, YAP can reprogram metabolism to enable liver growth [93]. Those discoveries demonstrated an indispensable role of YAP in metabolism regulation which is a key step in cachexia development.

However, the dysregulation of metabolism can perturb host immune to control cancer development. Several studies have demonstrated that glucose utilization of TILs may be impaired by glycolytic activities of cancer cells [94, 95]. Moreover, glucose is a critical substrate for T lymphocytes [96]. The demand for glucose supply is altered when Naïve T cell differentiates into effector T cells, which rely on a high intake of glucose to support proliferation and effector functions, such as cytotoxicity and cytokine production [97]. The role of CXCL13 in the network of YAP, cancer immune and cachexia is poorly understood. We speculate that the secreted CXCL13 in the YAP-pancreas model may induce immune cell infiltration to pancreatic microenvironment leading the initiation of pancreatic cancer as well as pre-cachexia. Future studies will be focusing on two aspects. Firstly, we will determine whether CXCL13 is a direct target of YAP. Secondly, how CXCL13 affects pancreas microenvironment and its role in pancreatic CAC will be determined. Unveiling the underline mechanism will lay a solid foundation in translating a new approach for immunoprevention in pancreatic CAC.

Figure 3-1. Generation of inducible pancreas-specific YAP overexpression.

(A). Schematic representation of approaches in generating transgenic mice. The pancreas-specific Cre recombinase (Ptf1α-cre) is used to activate reverse tetracycline controlled transactivator (rtTA) in Rosa-LSL-rtTA knock-in mice. When these 2 mouse strains are crossed to a tetO-YAP^{S127A} transgenic mice, and when the triple transgenic mice are subjected to Dox-induction, YAP can be expressed in a Dox-inducible fashion specific in pancreas. (B). Tetracycline-inducible conditional YAP expression system. Dox binding to rtTA leads to transcriptional activation of transgene, YAP.

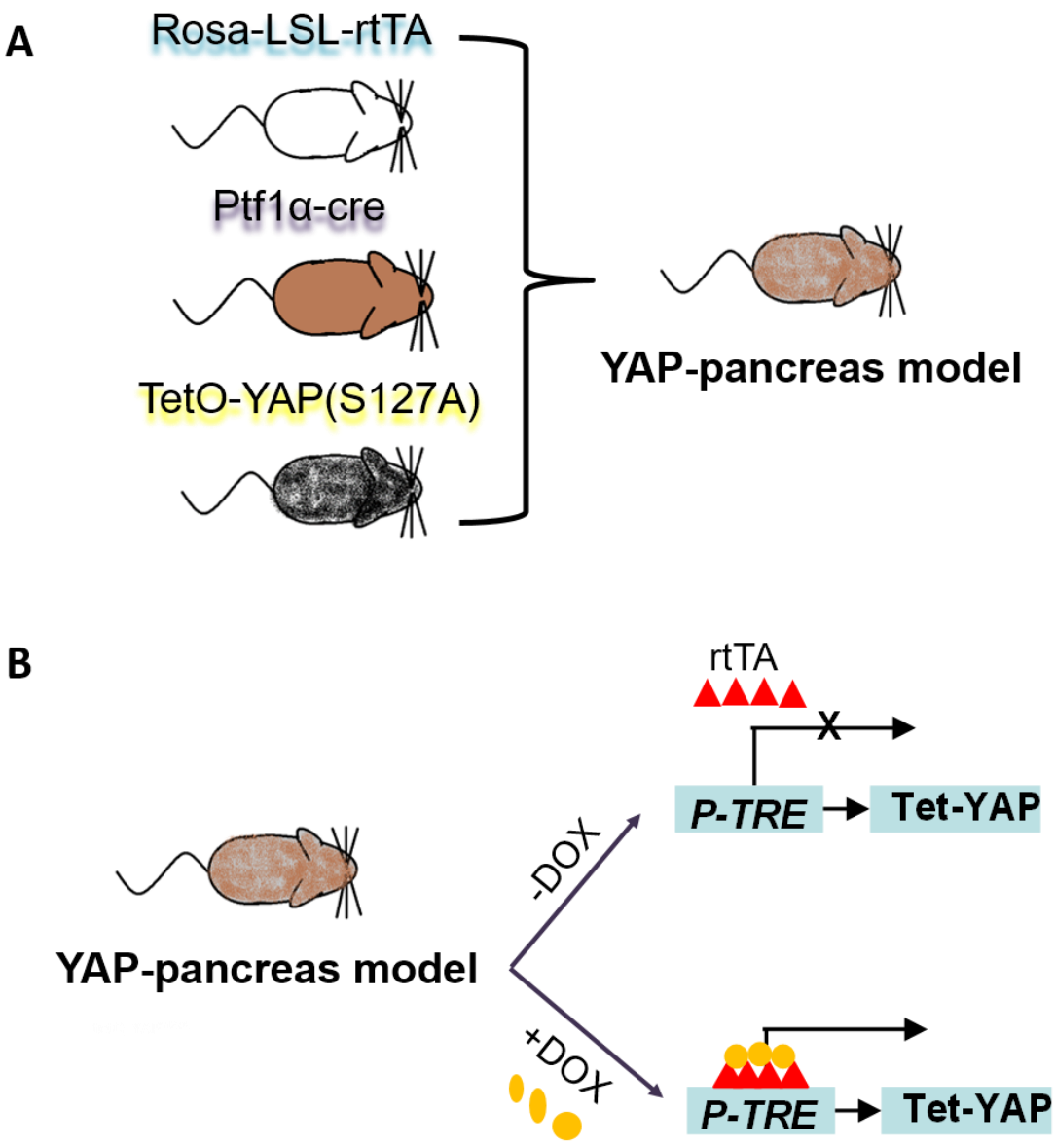
A
Rosa-LSL-rtTA
Ptf1α-cre
TetO-YAP(S127A)
YAP-pancreas model
B
rtTA
X
P-TRE
Tet-YAP
YAP-pancreas model
-DOX
+DOX
P-TRE
Tet-YAP

Figure 3-2. YAP is sufficient for ADM in YAP-Pancreas model.

(A-B) Representative images of H&E, YAP, Ki67, α-Amylase and CK19 IHC staining of pancreatic sections from 1-month-old control (CTRL, Ptf1a-Cre; Rosa-LSL-rtTA) and YAP transgenic (YAP-tg, Ptf1a-Cre; Rosa-LSL-rtTA;YAP^{S127A}) with 2 week dox induction. (C) Representative pancreas image from mice used in (A).

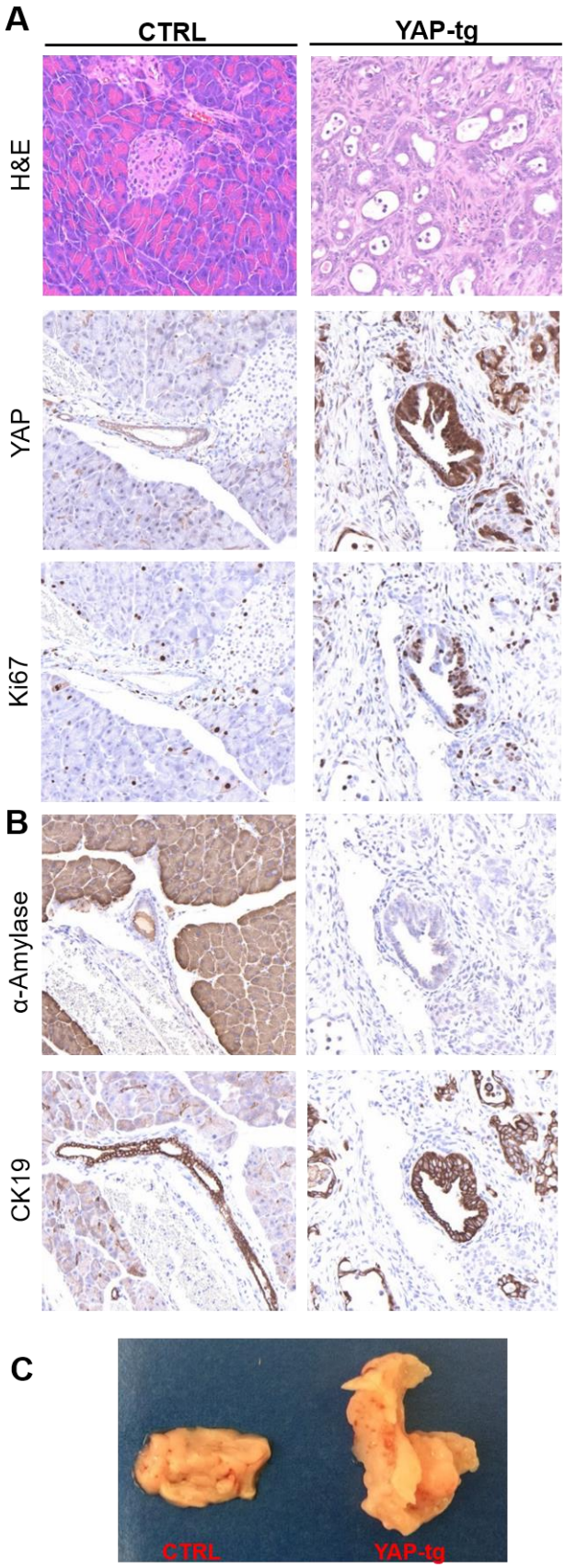
A
CTRL
YAP-tg
H&E
YAP
Ki67
B
α-Amylase
CK19
C
CTRL
YAP-tg

Figure 3-3. The YAP-Pancreas model has cachectic phenotype.

(A)Total body weight in YAP-pancreatic model and corresponding littermate controls of male and female (dox induction at 3-months age, n =3 per genotype) at the time point of 8 weeks after dox induction. (B-C) Food intake of mice used in (A). (D) Representative macroscopic pictures of control mice and YAP-pancreatic model with 2 weeks of dox induction at 1-month age at autopsy. The arrowheads point to normal left gonadal fat in control mice. In the YAP-pancreatic model, left gonadal fat (arrowhead) is almost completely absent. (E)Representative images of hematoxylin and eosin (H&E) staining of gonadal fat in mice from (D).

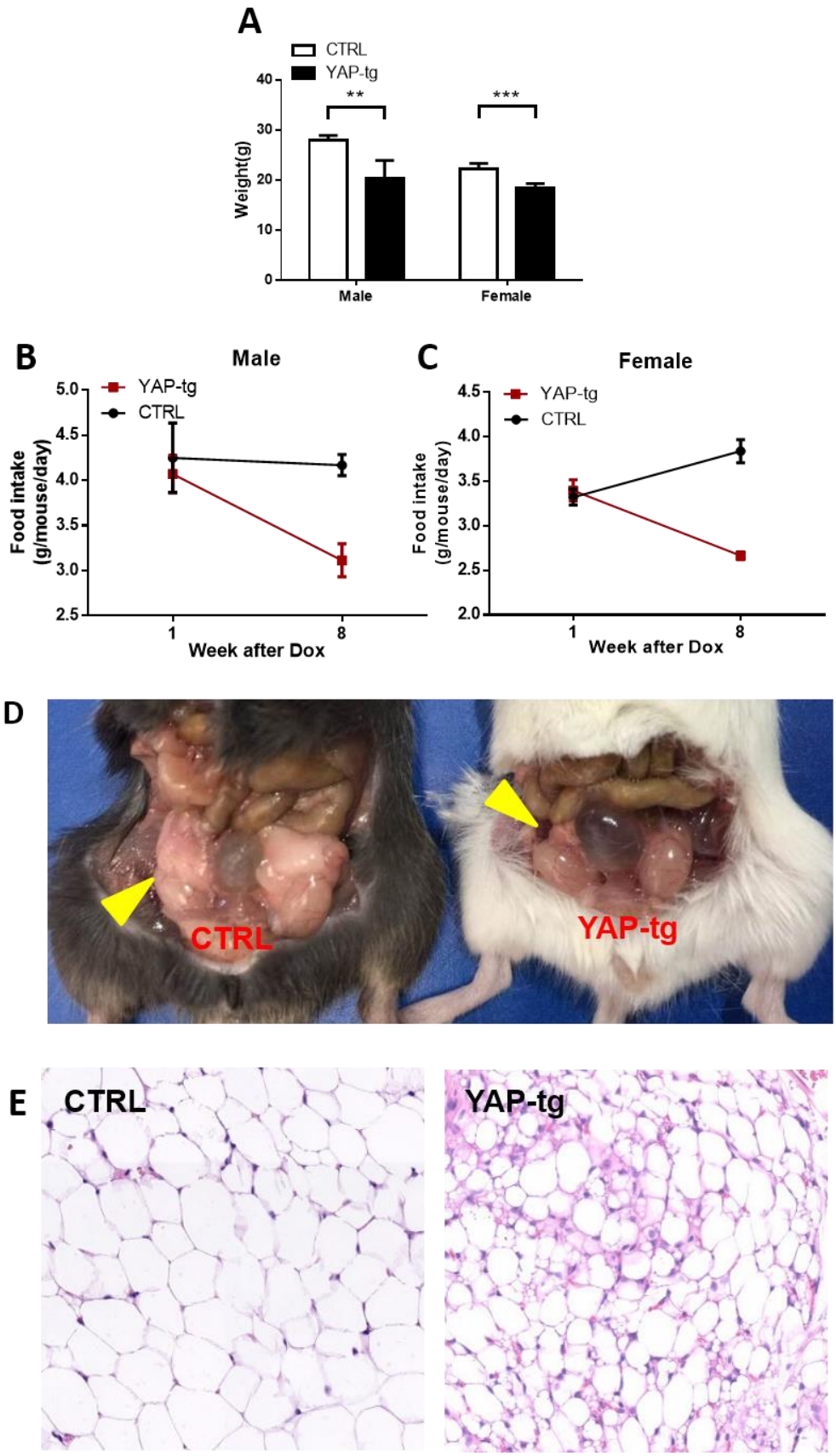
A
CTRL
YAP-tg
**
***
Weight(g)
40
30
20
10
0
Male
Female
B
Male
YAP-tg
CTRL
Food intake (g/mouse/day)
5.0
4.5
4.0
3.5
3.0
2.5
1
8
Week after Dox
C
Female
YAP-tg
CTRL
Food intake (g/mouse/day)
4.5
4.0
3.5
3.0
2.5
2.0
1
8
Week after Dox
D
CTRL
YAP-tg
E
CTRL
YAP-tg

Figure 3-4. CXCL13 is induced by YAP overexpression in pancreas.

(A) Proteome Profiler Mouse XL Cytokine Array results. CXCL13 dots are marked in red box. Other up-regulated factors are marked in blue box. (B) List of upregulated cytokines identified from (A). (C) ELISA measurements of CXCL13 relative protein level in YAP-pancreas mouse model serum.

A

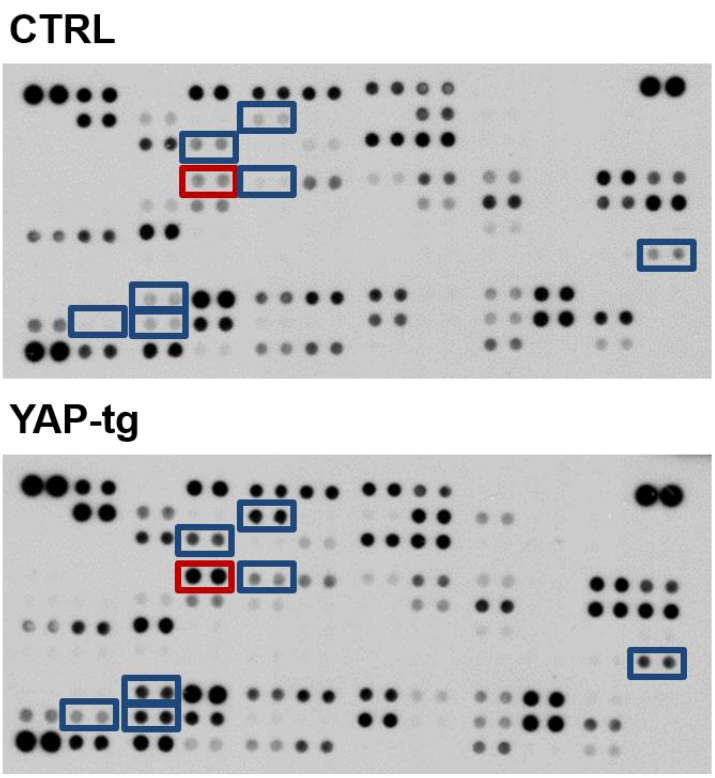

B

Gene Name	Description
CCL17/TARC 2	Thymus and activation-regulated chemokine 2
CHI3L1	Chitinase 3-like 1
CXCL13	C-X-C Motif Chemokine Ligand 13
CXCL16	C-X-C Motif Chemokine Ligand 16
LDL R	Low-Density Lipoprotein Receptor
Lipocalin-2/NGAL	Neutrophil gelatinase-associated lipocalin
Pentraxin 2/SAP 2	Sphingolipid activator protein-2
Pentraxin 3/TSG-14	TNF-inducible gene 14 protein

C

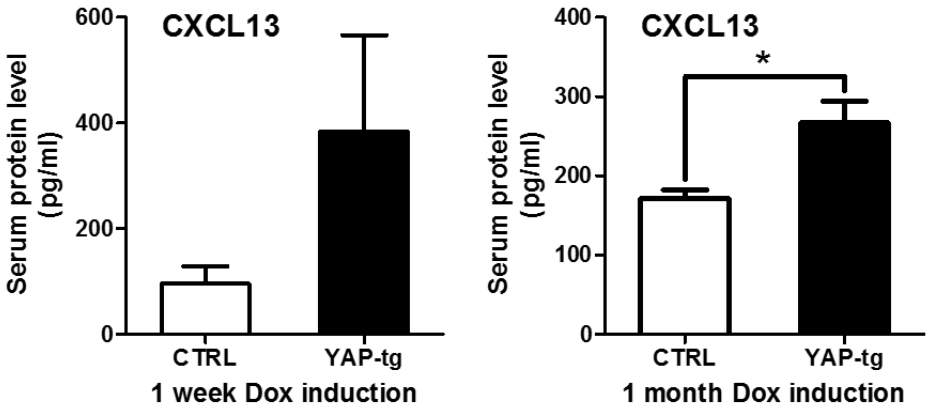

Table 1. List of genetic mouse strain source.

Strain symbol	Sources
Ptf1α-Cre	Mutant Mouse Resource & Research Centers
Rosa-LSL-rtTA	The Jackson Laboratory
TetO-YAP(S127A)	Harvard University, Dr. Fernando Carmago

BIBLIOGRAPHY

1. Pan, D., *Hippo signaling in organ size control.* Genes Dev, 2007. **21**(8): p. 886-97.
2. Pan, D., *The hippo signaling pathway in development and cancer.* Dev Cell, 2010. **19**(4): p. 491-505.
3. Harvey, K.F., X. Zhang, and D.M. Thomas, *The Hippo pathway and human cancer.* Nat Rev Cancer, 2013. **13**(4): p. 246-57.
4. Zhao, B., K. Tumaneng, and K.L. Guan, *The Hippo pathway in organ size control, tissue regeneration and stem cell self-renewal.* Nat Cell Biol, 2011. **13**(8): p. 877-83.
5. Yu, F.X., B. Zhao, and K.L. Guan, *Hippo Pathway in Organ Size Control, Tissue Homeostasis, and Cancer.* Cell, 2015. **163**(4): p. 811-28.
6. Moroishi, T., C.G. Hansen, and K.L. Guan, *The emerging roles of YAP and TAZ in cancer.* Nat Rev Cancer, 2015. **15**(2): p. 73-9.
7. Yu, F.X. and K.L. Guan, *The Hippo pathway: regulators and regulations.* Genes Dev, 2013. **27**(4): p. 355-71.
8. Piccolo, S., S. Dupont, and M. Cordenonsi, *The biology of YAP/TAZ: hippo signaling and beyond.* Physiol Rev, 2014. **94**(4): p. 1287-312.
9. Ma, B., et al., *Hypoxia regulates Hippo signalling through the SIAH2 ubiquitin E3 ligase.* Nat Cell Biol, 2015. **17**(1): p. 95-103.
10. Wang, W., et al., *AMPK modulates Hippo pathway activity to regulate energy homeostasis.* Nat Cell Biol, 2015. **17**(4): p. 490-9.
11. Mo, J.S., et al., *Cellular energy stress induces AMPK-mediated regulation of YAP and the Hippo pathway.* Nat Cell Biol, 2015. **17**(4): p. 500-10.
12. Yang, S., et al., *CDK1 phosphorylation of YAP promotes mitotic defects and cell motility and is essential for neoplastic transformation.* Cancer Res, 2013. **73**(22): p. 6722-33.
13. Yang, S., et al., *Oncoprotein YAP regulates the spindle checkpoint activation in a mitotic phosphorylation-dependent manner through up-regulation of BubR1.* J Biol Chem, 2015. **290**(10): p. 6191-202.
14. Ganem, N.J., et al., *Cytokinesis failure triggers hippo tumor suppressor pathway activation.* Cell, 2014. **158**(4): p. 833-48.
15. Zhang, L., et al., *CDK1 phosphorylation of TAZ in mitosis inhibits its oncogenic activity.* Oncotarget, 2015. **6**(31): p. 31399-412.
16. Hansen, C.G., T. Moroishi, and K.L. Guan, *YAP and TAZ: a nexus for Hippo signaling and beyond.* Trends Cell Biol, 2015. **25**(9): p. 499-513.
17. Das Thakur, M., et al., *Ajuba LIM proteins are negative regulators of the Hippo signaling pathway.* Curr Biol, 2010. **20**(7): p. 657-62.
18. Reddy, B.V. and K.D. Irvine, *Regulation of Hippo signaling by EGFR-MAPK signaling through Ajuba family proteins.* Dev Cell, 2013. **24**(5): p. 459-71.
19. Sun, G. and K.D. Irvine, *Ajuba family proteins link JNK to Hippo signaling.* Sci Signal, 2013. **6**(292): p. ra81.

20. Rauskolb, C., et al., *Cytoskeletal tension inhibits Hippo signaling through an Ajuba-Warts complex.* Cell, 2014. **158**(1): p. 143-56.

21. Schimizzi, G.V. and G.D. Longmore, *Ajuba proteins.* Curr Biol, 2015. **25**(11): p. R445-6.

22. Liang, X.H., et al., *LIM protein JUB promotes epithelial-mesenchymal transition in colorectal cancer.* Cancer Sci, 2014. **105**(6): p. 660-6.

23. Tanaka, I., et al., *LIM-domain protein AJUBA suppresses malignant mesothelioma cell proliferation via Hippo signaling cascade.* Oncogene, 2015. **34**(1): p. 73-83.

24. Gao, Y.B., et al., *Genetic landscape of esophageal squamous cell carcinoma.* Nat Genet, 2014. **46**(10): p. 1097-102.

25. *Comprehensive genomic characterization of head and neck squamous cell carcinomas.* Nature, 2015. **517**(7536): p. 576-82.

26. Sharp, T.V., et al., *The chromosome 3p21.3-encoded gene, LIMD1, is a critical tumor suppressor involved in human lung cancer development.* Proc Natl Acad Sci U S A, 2008. **105**(50): p. 19932-7.

27. Hirota, T., et al., *Aurora-A and an interacting activator, the LIM protein Ajuba, are required for mitotic commitment in human cells.* Cell, 2003. **114**(5): p. 585-98.

28. Abe, Y., et al., *LATS2-Ajuba complex regulates gamma-tubulin recruitment to centrosomes and spindle organization during mitosis.* FEBS Lett, 2006. **580**(3): p. 782-8.

29. Ferrand, A., et al., *Ajuba: a new microtubule-associated protein that interacts with BUBR1 and Aurora B at kinetochores in metaphase.* Biol Cell, 2009. **101**(4): p. 221-35.

30. Ji, M., et al., *Phospho-regulation of KIBRA by CDK1 and CDC14 phosphatase controls cell-cycle progression.* Biochem J, 2012. **447**(1): p. 93-102.

31. Xiao, L., et al., *KIBRA protein phosphorylation is regulated by mitotic kinase aurora and protein phosphatase 1.* J Biol Chem, 2011. **286**(42): p. 36304-15.

32. Dong, J., et al., *Elucidation of a universal size-control mechanism in Drosophila and mammals.* Cell, 2007. **130**(6): p. 1120-33.

33. Brattain, M.G., et al., *Heterogeneity of human colon carcinoma.* Cancer Metastasis Rev, 1984. **3**(3): p. 177-91.

34. Xiao, L., et al., *KIBRA regulates Hippo signaling activity via interactions with large tumor suppressor kinases.* J Biol Chem, 2011. **286**(10): p. 7788-96.

35. Gunn-Moore, F.J., et al., *A novel 4.1 ezrin radixin moesin (FERM)-containing protein, 'Willin'.* FEBS Lett, 2005. **579**(22): p. 5089-94.

36. Yang, S., et al., *Phosphorylation of KIBRA by the extracellular signal-regulated kinase (ERK)-ribosomal S6 kinase (RSK) cascade modulates cell proliferation and migration.* Cell Signal, 2014. **26**(2): p. 343-51.

37. Zhao, B., et al., *TEAD mediates YAP-dependent gene induction and growth control.* Genes Dev, 2008. **22**(14): p. 1962-71.

38. Zhang, L., et al., *KIBRA regulates aurora kinase activity and is required for precise chromosome alignment during mitosis.* J Biol Chem, 2012. **287**(41): p. 34069-77.

39. Aylon, Y., et al., *A positive feedback loop between the p53 and Lats2 tumor suppressors prevents tetraploidization.* Genes Dev, 2006. **20**(19): p. 2687-700.

40. Nigg, E.A., *Cellular substrates of p34(cdc2) and its companion cyclin-dependent kinases.* Trends Cell Biol, 1993. **3**(9): p. 296-301.

41. Hornbeck, P.V., et al., *PhosphoSitePlus, 2014: mutations, PTMs and recalibrations.* Nucleic Acids Res, 2015. **43**(Database issue): p. D512-20.

42. Lamouille, S., J. Xu, and R. Derynck, *Molecular mechanisms of epithelial-mesenchymal transition.* Nat Rev Mol Cell Biol, 2014. **15**(3): p. 178-96.

43. Kisseleva, M., et al., *The LIM protein Ajuba regulates phosphatidylinositol 4,5-bisphosphate levels in migrating cells through an interaction with and activation of PIPKI alpha.* Mol Cell Biol, 2005. **25**(10): p. 3956-66.

44. Holland, A.J. and D.W. Cleveland, *Boveri revisited: chromosomal instability, aneuploidy and tumorigenesis.* Nat Rev Mol Cell Biol, 2009. **10**(7): p. 478-87.

45. Mardin, B.R., et al., *Components of the Hippo pathway cooperate with Nek2 kinase to regulate centrosome disjunction.* Nat Cell Biol, 2010. **12**(12): p. 1166-76.

46. Nishio, M., et al., *Cancer susceptibility and embryonic lethality in Mob1a/1b double-mutant mice.* J Clin Invest, 2012. **122**(12): p. 4505-18.

47. Yabuta, N., et al., *Lats2 is an essential mitotic regulator required for the coordination of cell division.* J Biol Chem, 2007. **282**(26): p. 19259-71.

48. Hirota, T., et al., *Zyxin, a regulator of actin filament assembly, targets the mitotic apparatus by interacting with h-warts/LATS1 tumor suppressor.* J Cell Biol, 2000. **149**(5): p. 1073-86.

49. Gaedcke, J., et al., *Mutated KRAS results in overexpression of DUSP4, a MAP-kinase phosphatase, and SMYD3, a histone methyltransferase, in rectal carcinomas.* Genes Chromosomes Cancer, 2010. **49**(11): p. 1024-34.

50. Kaiser, S., et al., *Transcriptional recapitulation and subversion of embryonic colon development by mouse colon tumor models and human colon cancer.* Genome Biol, 2007. **8**(7): p. R131.

51. Hong, Y., et al., *A 'metastasis-prone' signature for early-stage mismatch-repair proficient sporadic colorectal cancer patients and its implications for possible therapeutics.* Clin Exp Metastasis, 2010. **27**(2): p. 83-90.

52. Skrzypczak, M., et al., *Modeling oncogenic signaling in colon tumors by multidirectional analyses of microarray data directed for maximization of analytical reliability.* PLoS One, 2010. **5**(10).

53. Zhou, D., et al., *Mst1 and Mst2 maintain hepatocyte quiescence and suppress hepatocellular carcinoma development through inactivation of the Yap1 oncogene.* Cancer Cell, 2009. **16**(5): p. 425-38.

54. Zhou, D., et al., *Mst1 and Mst2 protein kinases restrain intestinal stem cell proliferation and colonic tumorigenesis by inhibition of Yes-associated protein (Yap) overabundance.* Proc Natl Acad Sci U S A, 2011. **108**(49): p. E1312-20.

55. Lu, L., et al., *Hippo signaling is a potent in vivo growth and tumor suppressor pathway in the mammalian liver.* Proc Natl Acad Sci U S A, 2010. **107**(4): p. 1437-42.

56. Song, H., et al., *Mammalian Mst1 and Mst2 kinases play essential roles in organ size control and tumor suppression.* Proc Natl Acad Sci U S A, 2010. **107**(4): p. 1431-6.

57. Qin, F., et al., *Mst1 and Mst2 kinases: regulations and diseases.* Cell Biosci, 2013. **3**(1): p. 31.

58. Hanahan, D. and R.A. Weinberg, *Hallmarks of cancer: the next generation.* Cell, 2011. **144**(5): p. 646-74.

59. Oh, H.J., et al., *MST1 limits the kinase activity of aurora B to promote stable kinetochore-microtubule attachment.* Curr Biol, 2010. **20**(5): p. 416-22.

60. Mardin, B.R., et al., *Plk1 controls the Nek2A-PP1gamma antagonism in centrosome disjunction.* Curr Biol, 2011. **21**(13): p. 1145-51.

61. Chen, X., et al., *Ajuba Phosphorylation by CDK1 Promotes Cell Proliferation and Tumorigenesis.* J Biol Chem, 2016. **291**(28): p. 14761-72.

62. Zhao, B., et al., *Inactivation of YAP oncoprotein by the Hippo pathway is involved in cell contact inhibition and tissue growth control.* Genes Dev, 2007. **21**(21): p. 2747-61.

63. Kim, H., et al., *Wnt Signaling Translocates Lys48-Linked Polyubiquitinated Proteins to the Lysosomal Pathway.* Cell Rep, 2015. **11**(8): p. 1151-9.

64. Chiba, S., et al., *MST2- and Furry-mediated activation of NDR1 kinase is critical for precise alignment of mitotic chromosomes.* Curr Biol, 2009. **19**(8): p. 675-81.

65. Cooper, C., et al., *Understanding and managing cancer-related weight loss and anorexia: insights from a systematic review of qualitative research.* J Cachexia Sarcopenia Muscle, 2015. **6**(1): p. 99-111.

66. Fearon, K., J. Arends, and V. Baracos, *Understanding the mechanisms and treatment options in cancer cachexia.* Nat Rev Clin Oncol, 2013. **10**(2): p. 90-9.

67. Tisdale, M.J., *Cachexia in cancer patients.* Nat Rev Cancer, 2002. **2**(11): p. 862-71.

68. Landskron, G., et al., *Chronic inflammation and cytokines in the tumor microenvironment.* J Immunol Res, 2014. **2014**: p. 149185.

69. Salgado, R., et al., *Circulating interleukin-6 predicts survival in patients with metastatic breast cancer.* Int J Cancer, 2003. **103**(5): p. 642-6.

70. Petruzzelli, M., et al., *A switch from white to brown fat increases energy expenditure in cancer-associated cachexia.* Cell Metab, 2014. **20**(3): p. 433-47.

71. Lee, K.E., et al., *Hif1a Deletion Reveals Pro-Neoplastic Function of B Cells in Pancreatic Neoplasia.* Cancer Discov, 2016. **6**(3): p. 256-69.

72. Fearon, K.C., D.J. Glass, and D.C. Guttridge, *Cancer cachexia: mediators, signaling, and metabolic pathways.* Cell Metab, 2012. **16**(2): p. 153-66.

73. Bruera, E., *ABC of palliative care. Anorexia, cachexia, and nutrition.* BMJ, 1997. **315**(7117): p. 1219-22.

74. Dewys, W.D., et al., *Prognostic effect of weight loss prior to chemotherapy in cancer patients. Eastern Cooperative Oncology Group.* Am J Med, 1980. **69**(4): p. 491-7.

75. Zhang, W., et al., *Downstream of mutant KRAS, the transcription regulator YAP is essential for neoplastic progression to pancreatic ductal adenocarcinoma.* Sci Signal, 2014. **7**(324): p. ra42.

76. Justice, R.W., et al., *The Drosophila tumor suppressor gene warts encodes a homolog of human myotonic dystrophy kinase and is required for the control of cell shape and proliferation.* Genes Dev, 1995. **9**(5): p. 534-46.

77. Harvey, K. and N. Tapon, *The Salvador-Warts-Hippo pathway - an emerging tumour-suppressor network.* Nat Rev Cancer, 2007. **7**(3): p. 182-91.

78. Nguyen, L.T., et al., *ERG Activates the YAP1 Transcriptional Program and Induces the Development of Age-Related Prostate Tumors.* Cancer Cell, 2015. **27**(6): p. 797-808.

79. Yang, S., et al., *Active YAP promotes pancreatic cancer cell motility, invasion and tumorigenesis in a mitotic phosphorylation-dependent manner through LPAR3.* Oncotarget, 2015. **6**(34): p. 36019-31.

80. Kapoor, A., et al., *Yap1 activation enables bypass of oncogenic Kras addiction in pancreatic cancer.* Cell, 2014. **158**(1): p. 185-197.

81. Camargo, F.D., et al., *YAP1 increases organ size and expands undifferentiated progenitor cells.* Curr Biol, 2007. **17**(23): p. 2054-60.

82. Kern, K.A. and J.A. Norton, *Cancer cachexia.* JPEN J Parenter Enteral Nutr, 1988. **12**(3): p. 286-98.

83. Loberg, R.D., et al., *The lethal phenotype of cancer: the molecular basis of death due to malignancy.* CA Cancer J Clin, 2007. **57**(4): p. 225-41.

84. Tsoli, M. and G. Robertson, *Cancer cachexia: malignant inflammation, tumorkines, and metabolic mayhem.* Trends Endocrinol Metab, 2013. **24**(4): p. 174-83.

85. Gunn, M.D., et al., *A B-cell-homing chemokine made in lymphoid follicles activates Burkitt's lymphoma receptor-1.* Nature, 1998. **391**(6669): p. 799-803.

86. Gunderson, A.J., et al., *Bruton Tyrosine Kinase-Dependent Immune Cell Cross-talk Drives Pancreas Cancer.* Cancer Discov, 2016. **6**(3): p. 270-85.

87. Pylayeva-Gupta, Y., et al., *IL35-Producing B Cells Promote the Development of Pancreatic Neoplasia.* Cancer Discov, 2016. **6**(3): p. 247-55.

88. Koizumi, M., et al., *Increased B cell-activating factor promotes tumor invasion and metastasis in human pancreatic cancer.* PLoS One, 2013. **8**(8): p. e71367.

89. Moroishi, T., et al., *The Hippo Pathway Kinases LATS1/2 Suppress Cancer Immunity.* Cell, 2016. **167**(6): p. 1525-1539 e17.

90. Guo, X., et al., *Single tumor-initiating cells evade immune clearance by recruiting type II macrophages.* Genes Dev, 2017. **31**(3): p. 247-259.

91. Wang, G., et al., *Targeting YAP-Dependent MDSC Infiltration Impairs Tumor Progression.* Cancer Discov, 2016. **6**(1): p. 80-95.

92. Sorrentino, G., et al., *Metabolic control of YAP and TAZ by the mevalonate pathway.* Nat Cell Biol, 2014. **16**(4): p. 357-66.

93. Wang, Z., et al., *Interplay of mevalonate and Hippo pathways regulates RHAMM transcription via YAP to modulate breast cancer cell motility.* Proc Natl Acad Sci U S A, 2014. **111**(1): p. E89-98.

94. Chang, C.H., et al., *Metabolic Competition in the Tumor Microenvironment Is a Driver of Cancer Progression.* Cell, 2015. **162**(6): p. 1229-41.

95. Ho, P.C., et al., *Phosphoenolpyruvate Is a Metabolic Checkpoint of Anti-tumor T Cell Responses.* Cell, 2015. **162**(6): p. 1217-28.

96. Greiner, E.F., M. Guppy, and K. Brand, *Glucose is essential for proliferation and the glycolytic enzyme induction that provokes a transition to glycolytic energy production.* J Biol Chem, 1994. **269**(50): p. 31484-90.

97. Gerriets, V.A., et al., *Metabolic programming and PDHK1 control CD4+ T cell subsets and inflammation.* J Clin Invest, 2015. **125**(1): p. 194-207.